

Chiral and Regenerable NAD(P)H Models Enabled Biomimetic Asymmetric Reduction: Design, Synthesis, Scope, and Mechanistic Studies

Jie Wang,[§] Zi-Biao Zhao,[§] Yanan Zhao, Gen Luo, Zhou-Hao Zhu, Yi Luo,^{*} and Yong-Gui Zhou^{*}



Cite This: *J. Org. Chem.* 2020, 85, 2355–2368



Read Online

ACCESS |



Metrics & More

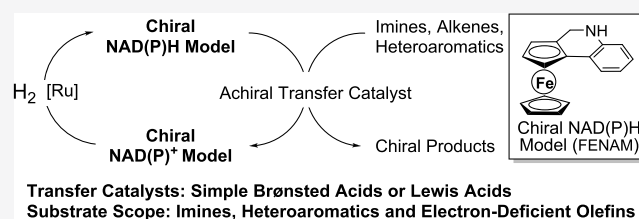


Article Recommendations



Supporting Information

ABSTRACT: The coenzyme NAD(P)H plays an important role in electron as well as proton transmission in the cell. Thus, a variety of NAD(P)H models have been involved in biomimetic reduction, such as stoichiometric Hantzsch esters and achiral regenerable dihydrophenanthridine. However, the development of a general and new-generation biomimetic asymmetric reduction is still a long-term challenge. Herein, a series of chiral and regenerable NAD(P)H models with central, axial, and planar chiralities have been designed and applied in biomimetic asymmetric reduction using hydrogen gas as a terminal reductant. Combining chiral NAD(P)H models with achiral transfer catalysts such as Brønsted acids and Lewis acids, the substrate scope could be also expanded to imines, heteroaromatics, and electron-deficient tetrasubstituted alkenes with up to 99% yield and 99% enantiomeric excess (ee). The mechanism of chiral regenerable NAD(P)H models was investigated as well. Isotope-labeling reactions indicated that chiral NAD(P)H models were regenerated by the ruthenium complex under hydrogen gas first, and then the hydride of NAD(P)H models was transferred to unsaturated bonds in the presence of transfer catalysts. In addition, density functional theory calculations were also carried out to give further insight into the transition states for the corresponding transfer catalysts.



INTRODUCTION

As a pair of the most significant coenzymes found in the biological cell, the reduced nicotinamide adenine dinucleotide (NADH) and nicotinamide adenine dinucleotide phosphate (NADPH) play important roles in metabolism processes and over 400 enzyme redox reactions. All of these processes and reactions entirely depend on the interconversion of NAD(P)H and NAD(P)⁺ (Scheme 1a).¹ Therefore, the development of NAD(P)H models has attracted much attention and gradually become one of the most important fields in biomimetic asymmetric reduction (BMAR).

In the past decades, numerous novel NAD(P)H models have been designed and involved in biomimetic asymmetric reduction. Earlier NAD(P)H models mainly focused on the chiral dihydronicotinamide derivatives and realized asymmetric reduction of ketones in the presence of the stoichiometric Lewis acids.² Meanwhile, earlier NAD(P)H models are designed primarily by the following three aspects: introduce a remote sterically demanding side chain to the structure, change the different substituents at 4-position of the dihydropyridine ring, and design a special conformation to obtain stereoselectivity.^{2a,b} Subsequently, Hantzsch esters (HEHs)³ and benzothiazolines⁴ as the representatives of the NAD(P)H models have been successfully employed in biomimetic asymmetric reduction of a variety of unsaturated compounds, using the chiral organocatalysts⁵ and metal catalysts⁶ as transfer catalysts (Scheme 1b). However, these

reactions required stoichiometric amounts of NAD(P)H models, and there were inevitable limitations in regeneration,⁷ leading to low atomic economy and difficulty in product isolation. Recently, our group reported biomimetic asymmetric hydrogenation of imines and heteroaromatics with chiral phosphoric acids and catalytic amounts of achiral dihydrophenanthridine (DHPD).⁸ Achiral DHPD could be easily regenerated under hydrogen gas using homogeneous ruthenium.⁸ Later, Beller's group found that DHPD could be regenerated under iron catalysts and realized the biomimetic asymmetric reduction of imines (Scheme 1c).⁹ Although much significant progress has been achieved in the design of NAD(P)H models, the development of a general and new-generation biomimetic asymmetric reduction process is still a major challenge in the area of biomimetic asymmetric catalysis.

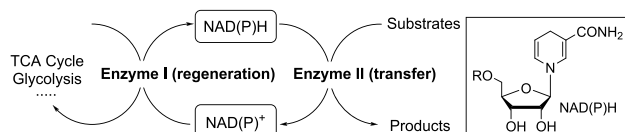
For early works about biomimetic asymmetric reduction concentrated on achiral regenerable NAD(P)H models, the element of stereocontrol is the chiral transfer catalyst, mainly chiral Brønsted acids.^{3–6} Although it has gained great progress, tedious screening of chiral transfer catalysts has to be carried out for every biomimetic reduction. Recently, our group

Received: November 13, 2019

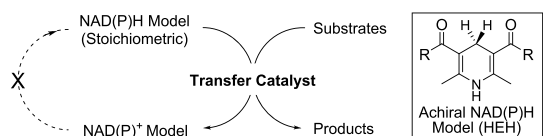
Published: December 30, 2019

Scheme 1. Biomimetic Asymmetric Reduction (BMAR) Based on the Coenzyme NAD(P)H

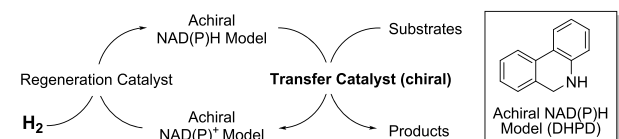
a. NAD(P)H-mediated metabolism process in the cell



b. Biomimetic asymmetric reduction with **stoichiometric** NAD(P)H models

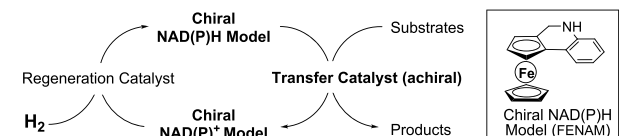


c. Biomimetic asymmetric reduction with **regenerable** NAD(P)H models



This Work: New Generation of Biomimetic Asymmetric Reduction

d. Biomimetic reduction with **chiral and regenerable** NAD(P)H models



- A general biomimetic asymmetric reduction process using hydrogen
- Transfer catalysts: Brønsted acid or Lewis acid
- Substrate scope: imines, heteroaromatics and alkenes

reported a chiral and regenerable NAD(P)H model, which facilitated biomimetic asymmetric reduction using the Lewis acid as the transfer catalyst.¹⁰ However, there are still some issues to be noted in these reactions. First, the detailed mechanism of the chiral regenerable NAD(P)H model-facilitated biomimetic asymmetric reduction remains to be elucidated, in terms of the fashion of hydride transfer. Second, the interaction among the NAD(P)H model, transfer catalyst, and substrate was relatively unexplored. Third, the substrate scope based on the chiral regenerable NAD(P)H model should be further investigated.

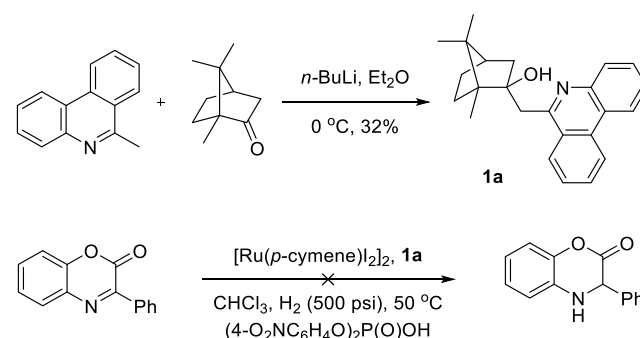
In this article, we systematically examined various chiral regenerable NAD(P)H models with central, axial, and planar chiralities. Brønsted acids and Lewis acids could be regarded as transfer catalysts to realize biomimetic asymmetric reduction. The substrate scope could be extremely expanded to imines, heteroaromatics, and alkenes with excellent activities and enantioselectivities. In addition, we also gain insight into the detailed mechanism of chiral regenerable NAD(P)H model-facilitated biomimetic asymmetric reduction by a combination of experimental and theoretical studies.

RESULTS AND DISCUSSION

Synthesis of a Chiral and Regenerable NAD(P)H Model with Central Chirality. Our previous studies have demonstrated that 9,10-dihydrophenanthridine is easily regenerable and efficient in the hydride transfer process. Thus, we first focused on the study about the property of the centrally chiral NAD(P)H model **1a** containing the key structure phenanthridine, which could be easily synthesized from 6-methylphenanthridine and naturally occurring chiral

ketone camphor in one step with 32% yield. Next, the regeneration was conducted under hydrogen gas with a homogeneous ruthenium catalyst; the reaction proceeded smoothly, giving the reductive form with 46% yield. However, biomimetic asymmetric reduction could not proceed with the homogeneous ruthenium complex and simple phosphoric acid as the regeneration and transfer catalysts, respectively, mainly due to the bulky steric hindrance and intramolecular hydrogen bonding between hydroxyl and nitrogen atoms, resulting in the difficulty in the hydride transfer process (Scheme 2). So, for the rationale design of the chiral and regenerable NAD(P)H model, there can be no substituent at the active site of the NAD(P)H model.

Scheme 2. Chiral and Regenerable NAD(P)H Model: Initial Experiments



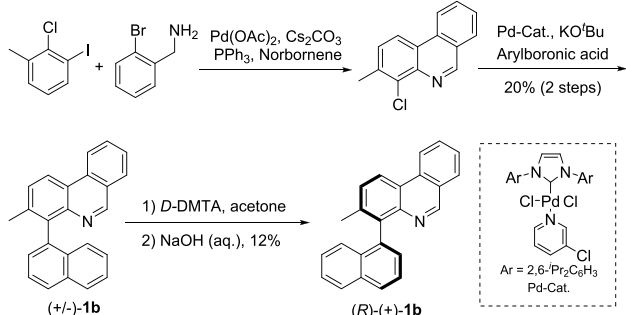
Synthesis of Chiral and Regenerable NAD(P)H Models with Axial Chirality. Then, we turned our attention to NAD(P)H models with axial chirality. Racemic axially chiral phenanthridines **1b** and **1c** (Scheme 3) could be synthesized by Suzuki coupling of the halogen-substituted phenanthridine with aryl boronic acid, followed by chemical resolution by D-tartaric acid derivatives (D-DMTAs).¹¹ To confirm the validity of axially chiral NAD(P)H models, quinoxalinone **3a** was chosen as the model substrate¹² for biomimetic asymmetric reduction with the commercially available achiral diphenyl hydrogen phosphate **2a** as the transfer catalyst (Table 1). Unfortunately, no desired product was observed using (R)-**1b** and (R)-**1c** (Table 1, entries 1 and 2). The reason might be that the nitrogen atom was too close to the C2 axial stereocenter, impeding the formation of the hydrogen-bonding interaction with the substrate. Subsequently, the axially chiral NAD(P)H model (R)-**1d** involving the nitrogen far away from the axial stereogenic center was synthesized with 2-amino-6-bromobenzaldehyde as the starting material (Scheme 4). As expected, the desirable product **4a** was afforded with poor 16% enantiomeric excess (ee) at 12% conversion (Table 1, entry 3). Changing the methyl group to methoxyl (S)-**1e**, the enantioselectivity increased to moderate 50% ee and 22% conversion, but it was still difficult to improve the reactivity and enantioselectivity further (Table 1, entry 4).

Although only moderate enantioselectivity and reactivity were obtained, these experimental results demonstrated the feasibility in biomimetic asymmetric reduction with the regenerable and chiral NAD(P)H models. Achiral and simple phosphoric acid derivatives could also be used as transfer catalysts. The next step is to design and synthesize new and more efficient chiral and regenerable NAD(P)H models.

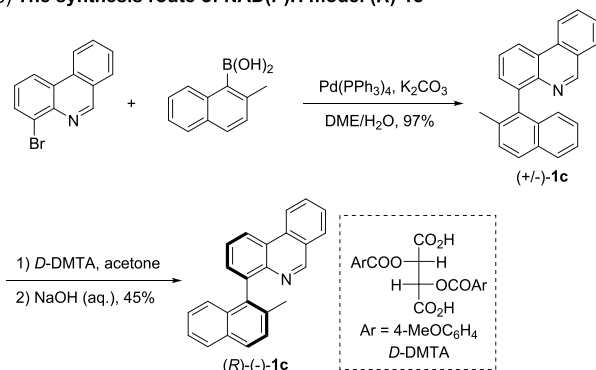
Synthesis of Chiral and Regenerable NAD(P)H Models with Planar Chirality. Since the discovery of

Scheme 3. Chiral NAD(P)H Model: N Atom Close to the C2 Axis

(a) The synthesis route of NAD(P)H model (R)-1b



(b) The synthesis route of NAD(P)H model (R)-1c



ferrocene in the 1950s,^{13a,b} chiral ferrocenyl compounds have been extensively applied in asymmetric catalysis. Among various areas, chiral ferrocene ligands are the most prominent. A wide variety of chiral ferrocenyl ligands are known today such as the Josiphos ligand and the Walphos and phosphite-oxazoline ligand-based ferrocene structure.^{13d–f} Besides, planar chiral heterocycles have been used in not only transition-metal catalysis but also nucleophilic catalysis.^{13c,f} Inspired by the extensive application of planar chirality in asymmetric synthesis, we wondered if the planar chiral framework would achieve a better stereoselective control, taking advantage of steric resistance between its two sides. Therefore, NAD(P)H models with planar chirality based on the ferrocene framework were designed. Combined with previous experience, new NAD(P)H models should be no substituents on the active site. In addition, the nitrogen atom should be far away from the planar stereogenic center. According to the known literature,^{10,14} starting with the readily available ferrocenealdehyde, a series of chiral regenerable ferrocene-based NAD(P)H models (abbreviated as FENAM) (R)-1f–i with various electronic properties could be synthesized in moderate total yields (Scheme 5).

Brønsted Acid Promoted BMAR. Gratifyingly, employing (R)-1f as the chiral and regenerable NAD(P)H model, the enantioselectivity could be dramatically improved to 97% ee. In this reaction, the homogeneous ruthenium complex could act as the regeneration catalyst and simple phosphoric acid could act as the transfer catalyst (Table 1, entry 5). Then, various solvents such as ethyl acetate, toluene, chloroform, and methanol were examined; the solvent chloroform proved to be the best (entries 5–10). After this, an array of Brønsted acids was extensively tested (entries 11–14). Besides, the planar chiral NAD(P)H models with different electronic properties

Table 1. Optimization of Brønsted Acid Promoted BMAR of Quinoxalinones^a

entry	solvent	acid 2	1	conv. (%) ^b	ee (%) ^c
1	CHCl ₃	2a	(R)-1b	<5	
2	CHCl ₃	2a	(R)-1c	<5	
3	CHCl ₃	2a	(R)-1d	12	16
4	CHCl ₃	2a	(S)-1e	22	50
5	CHCl ₃	2a	(R)-1f	78	97
6	CH ₂ Cl ₂	2a	(R)-1f	70	95
7	THF	2a	(R)-1f	<5	
8	EtOAc	2a	(R)-1f	<5	
9	toluene	2a	(R)-1f	35	90
10	MeOH	2a	(R)-1f	86	20
11	CHCl ₃	2b	(R)-1f	62	98
12	CHCl ₃	2c	(R)-1f	53	97
13	CHCl ₃	2d	(R)-1f	<5	
14	CHCl ₃	2e	(R)-1f	69	98
15 ^d	CHCl ₃	2a	(R)-1f	>95	97
16 ^d	CHCl ₃	2a	(R)-1g	>95 (96) ^e	98
17 ^d	CHCl ₃	2a	(R)-1h	>95	98
18 ^d	CHCl ₃	2a	(R)-1i	92	96

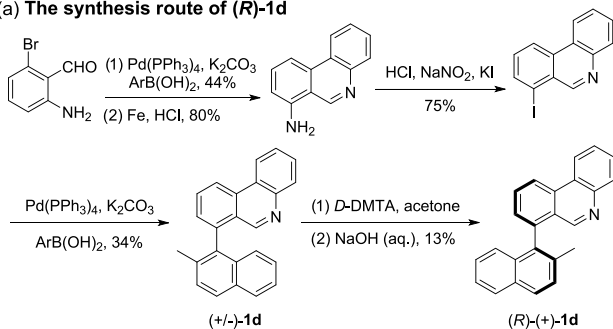
^aReaction conditions: 3a (0.1 mmol), [Ru(*p*-cymene)I₂]₂ (0.5 mol %), 1 (10 mol %), acid 2 (4 mol %), solvent (2 mL), H₂ (500 psi), 40 °C, 22 h. ^bConversion was measured by analysis of ¹H NMR spectra. ^cThe ee values were determined by chiral high-performance liquid chromatography (HPLC). ^dReaction time was prolonged to 48 h. ^eIsolated yield.

have a marginal beneficial effect (entries 15–18). Full conversion would be achieved while prolonging the time. Thus, the optimal protocol was identified: imine 3a (1.0 equiv.), [Ru(*p*-cymene)I₂]₂ (0.5 mol %), the chiral NAD(P)H model (R)-1g (10 mol %), achiral transfer catalyst Brønsted acid 2a (4 mol %), H₂ (500 psi), CHCl₃, and 40 °C.

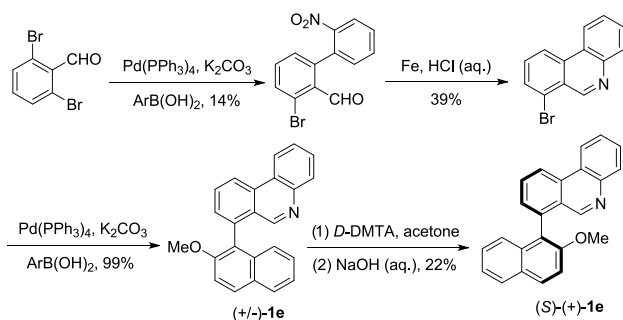
With the optimized conditions in hand, the substrate scope of the biomimetic asymmetric reduction was investigated using a catalytic amount of the chiral and regenerable NAD(P)H model. Gratifyingly, this strategy was suitable for a series of quinoxalinones with high activities and excellent enantioselectivities (92–98% yield, 96–99% ee). As depicted in Scheme 6, the electronic nature and steric effect on the phenyl of the substrate rarely influenced the reactivity and enantioselectivity, giving the desired reductive products in high enantioselectivities and yields (4a–f, 97–99% ee). Furthermore, benzyl- or allyl-protected substrates performed well with excellent results (4g, 4h). In the previous reports, the 3-alkyl-substituted quinoxalinones were much more challengeable, and low enantioselectivities were obtained (4i, 8% ee in ref 12b). It should be pointed out that the substituents at 3-position of quinoxalinones were not confined to the aryl groups, and 3-alkyl groups could also be tolerated to afford the desirable

Scheme 4. Chiral NAD(P)H Model: N Atom Far Away from the C2 Axis

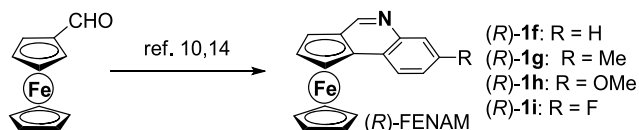
(a) The synthesis route of (R)-1d



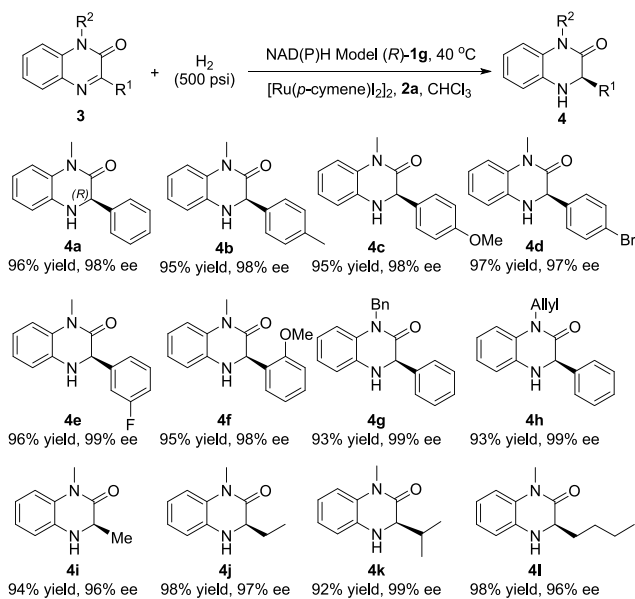
(b) The synthesis route of (S)-1e



Scheme 5. NAD(P)H Models with Planar Chirality



Scheme 6. Brønsted Acid Promoted BMAR of Quinoxalinones

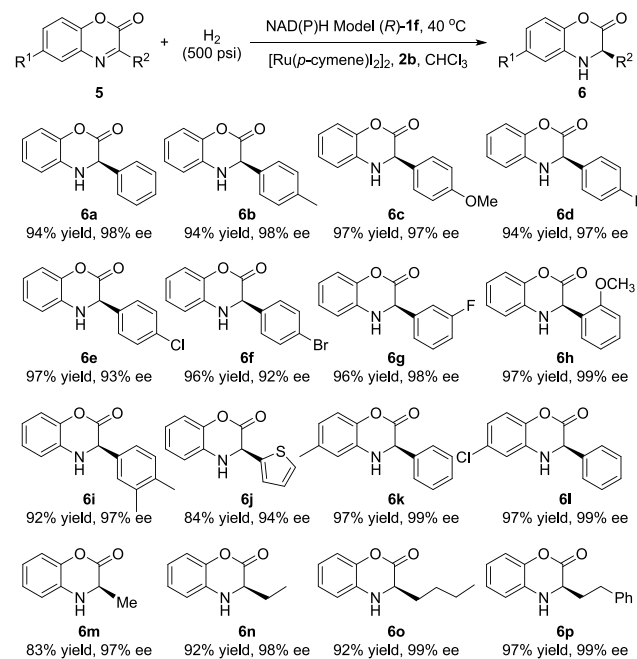


products with excellent activities and enantioselectivities (4i–l, 96–99% ee).

To expand the generality of this strategy, we next focused on the synthesis of the optically pure dihydrobenzoxazinones, which represent the crucial structural motif of bioactive

molecules and clinical pharmaceuticals.¹⁵ High activities and excellent enantioselectivities were obtained with most substrates (Scheme 7, 6a–p). The steric hindrance of the

Scheme 7. Brønsted Acid Promoted the BMAR of Benzoxazinones



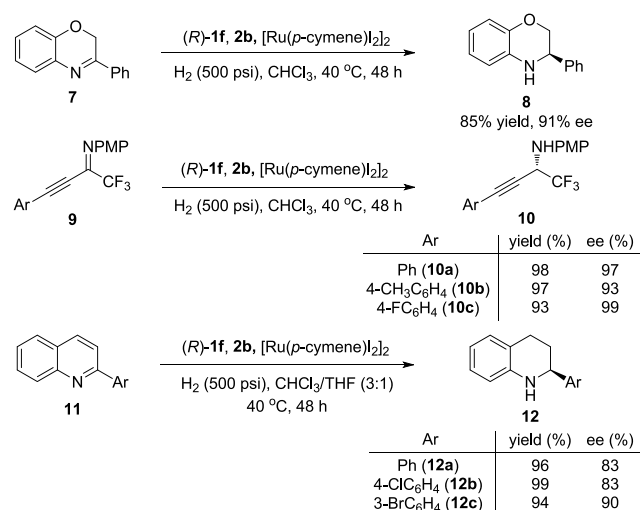
substituents on the phenyl appeared to have a marginal effect on the results. Besides, this protocol was also suitable for the substrates bearing halogen atoms (6d–f, 92–97% ee), which provides an opportunity for late-stage transformations. In addition, introducing a heteroaryl group onto the 3-position, the reaction also proceeded smoothly with excellent enantioselectivity (6j, 94% ee). Gratifyingly, switching aryl to alkyl groups, the substrates also participated well regardless of the length of the alkyl chain (6m–p, 97–99% ee).

To further showcase the utility of this strategy, we expanded the biomimetic asymmetric reduction to the benzoxazine,¹⁶ linear alkynyl ketimines,¹⁷ and heteroaromatic quinolines¹⁸ (Scheme 8). The reactions transformed smoothly, affording the corresponding chiral dihydrobenzoxazine 8, alkynyl amines 10, and tetrahydroquinolines 12 in good to excellent enantioselectivities.

Lewis Acid Promoted BMAR. Lewis acids could efficiently promote various organic reactions by coordination activation.¹⁹ Combined with chiral ligands, chiral Lewis acid catalysts could realize a myriad of asymmetric reactions. However, owing to electron-donating properties of chiral ligands, the decrease of the Lewis acidity ineluctably results in low coordination activation with the substrates, which limited its further application. Encouraged by the excellent results achieved by chiral and regenerable NAD(P)H models with achiral bench-stable Brønsted acid as the transfer catalyst, we postulated that the chiral regenerable NAD(P)H models would provide a new opportunity to simple Lewis acid, which may be regarded as the transfer catalyst as well to realize the biomimetic asymmetric reduction without the combination with chiral ligands to provide the chiral environment.

As challenging substrates in asymmetric catalysis, tetrasubstituted alkenes have attracted widespread attention for

Scheme 8. Brønsted Acid Promoted the BMAR of Other Imines and Heteroaromatics



scientific researchers, especially in biomimetic asymmetric reduction.²⁰ To our delight, simple commercially available Lewis acids could enable biomimetic asymmetric reduction of the tetrasubstituted alkenes 13. Different Lewis acids have different acidities, so the product ratio of 14a/14aa is different. After extensive screening of various Lewis acids, we found that readily available rare-earth ytterbium triflate [Yb(OTf)₃] afforded the optimal results in view of both activity and enantioselectivity (Table 2). It was observed that the

Table 2. Optimization of Lewis Acid-Promoted BMAR of Tetrasubstituted Alkenes^a

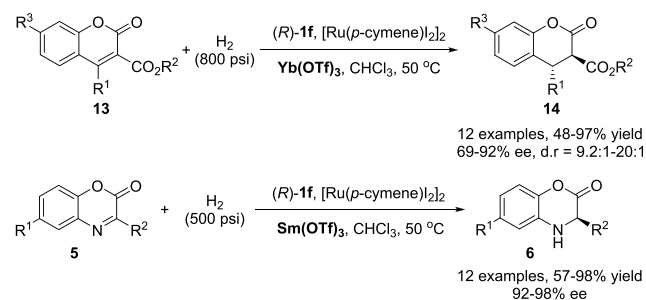
entry	LA	1	conv. (%) ^b	14a/14aa	14a ee (%) ^c
1	Sm(OTf) ₃	(R)-1c	4	>20:1	42
2	Sm(OTf) ₃	(S)-1e	40	>20:1	38
3	Sm(OTf) ₃	(R)-1f	11	10:1	87
4	Sm(OTf) ₃	(R)-1g	7	6.3:1	84
5	Sm(OTf) ₃	(R)-1h	8	11:1	76
6	Cu(OTf) ₂	(R)-1f	<5		
7	Sc(OTf) ₃	(R)-1f	<5		
8	Yb(OTf) ₃	(R)-1f	>95 (97 ^d)	>20:1	90
9		(R)-1f	<5		

^aReaction conditions 13a (0.10 mmol), [Ru(*p*-cymene)I₂]₂ (0.5 mol %), 1 (10 mol %), Lewis acid (20 mol %), CHCl₃ (2 mL), H₂ (800 psi), 50 °C. ^bConversion was measured by analysis of ¹H NMR spectra of unpurified mixtures and 14a d.r. > 20:1. ^cThe ee values were determined by HPLC analysis. ^dIsolated yield for the reaction with 0.15 mmol scale for 80 h.

thermodynamically controlled product, 3,4-trans-disubstituted dihydrocoumarins, could be achieved for aryl groups in excellent diastereoselectivities [diastereomeric ratio (d.r.) > 20:1] and enantioselectivities. The ratio of the main product 14a to the deacidified product 14aa was >20:1 with Yb(OTf)₃ as the transfer catalyst. As for the alkyl-substituted substrate, the desired products with moderate diastereo- and enantioselectivities could also be obtained.¹⁰ In addition, this strategy

was also suitable for the biomimetic asymmetric reduction of 3-aryl- and 3-alkyl-substituted benzoxazinones using Lewis acid Sm(OTf)₃ instead of Yb(OTf)₃ as the transfer catalyst, giving the desired products up to 98% ee and up to 98% yields (Scheme 9).¹⁰

Scheme 9. Lewis Acid Promoted BMAR of Tetrasubstituted Alkenes and Benzoxazinones

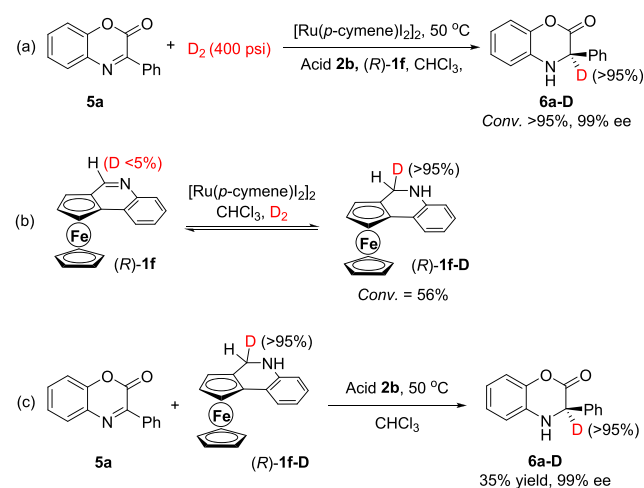


MECHANISTIC STUDY

Nonlinear Effect. To further understand the mechanism of the detailed reaction process, we examined the relationship between the ee value of the chiral NAD(P)H model and the reduced product 6a. It was indicated that the enantiomeric excess of the reductive product 6a was completely proportional to the enantiomeric excess of the chiral NAD(P)H model (R)-1f. The linear effect supported that the chiral NAD(P)H model for asymmetric induction was consistent with the 1:1 ratio of the substrate in the transition state.

Isotope-Labeling Experiments. To investigate the reaction pathway, several interrelated isotopic-labeling experiments were also conducted, as summarized in Scheme 10.

Scheme 10. Isotopic Labeling Experiments



Substrate 5a could be reduced under a D₂ atmosphere, affording the reductive deuterium product 6a-D. It was indicated that D₂ was the terminal reductant in the biomimetic reduction reaction (Scheme 10a). Meanwhile, the chiral and regenerable NAD(P)H model (R)-1f could be mildly regenerated with 56% conversion in the presence of D₂, and the deuterium atom was added to the less steric face (Scheme 10b). No deuterium atom incorporation was observed in the recovered NAD(P)H model (R)-1f. Treatment of substrate 5a

with the reductive NAD(P)H model (*R*)-1f-D led to the reductive product 6a-D with 95% deuterium incorporation and 99% ee (Scheme 10c). The result showed that the deuterium-incorporated chiral reductive NAD(P)H model (*R*)-1f-D could enantioselectively transfer deuterium to the imine 5a in the presence of Brønsted acid, and the deuterium atom on the less steric face was selectively transferred, leading to the excellent enantioselectivity.

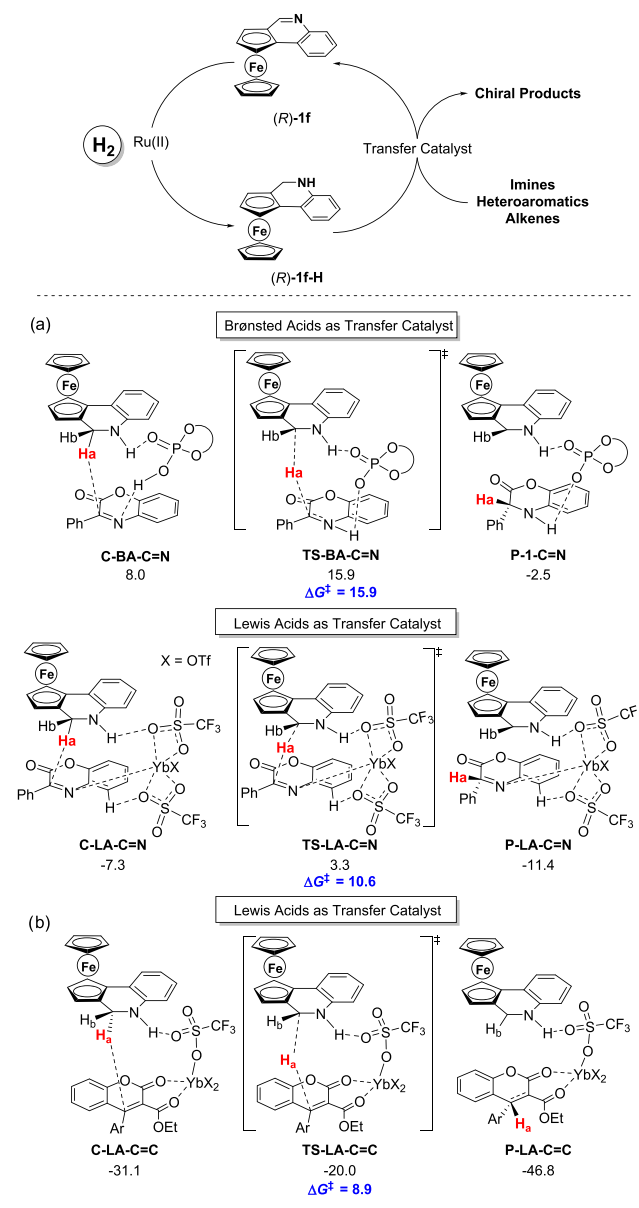
Isotopic-labeling experiments and the nonlinear effect have revealed the hydride transfer process in biomimetic asymmetric reduction. However, the detailed interaction among the chiral NAD(P)H models, substrates, and the transfer catalyst was not fully understood. Thus, the detailed mechanism was further studied by the density functional theory (DFT) calculations.

Density Functional Theory Calculations. On the basis of density functional theory calculations [see the Supporting Information (SI) for more details] and aforementioned experimental data, a plausible mechanism²¹ and optimized stationary points together with their relative energies are illustrated in Scheme 11.²² The optimized stationary points and relative energies mainly involved in the chiral and regenerable NAD(P)H model-facilitated biomimetic asymmetric reduction of C=N and C=C bonds. At first, the chiral NAD(P)H model (*R*)-1f could be reduced to (*R*)-1f-H in situ by the ruthenium complex and hydrogen gas. Then, the reduced chiral NAD(P)H model (*R*)-1f-H could realize biomimetic asymmetric reduction of C=C, C=N, and heteroaromatics with achiral transfer catalysts (Brønsted acid and Lewis acid). In the case of C=N bond reduction by Brønsted acid (ArO)₂P(O)OH (Scheme 11a), the transfer catalyst assists in the asymmetric reduction via forming O⋯H and N⋯H dual hydrogen-bond interactions with the chiral NAD(P)H model and 5a, respectively. This process has an energy barrier of 15.9 kcal/mol and is exergonic by 2.5 kcal/mol. In comparison, if the transfer catalyst is replaced by Lewis acid Yb(OTf)₃, the coordination of 5a via its N atom to the Yb center of Yb(OTf)₃ forms the complex C-LA-C=N with a relative energy of -7.3 kcal/mol, which surmounts an energy barrier of 10.6 kcal/mol (TS-LA-C=N) to give P-LA-C=N with a relative energy of -11.4 kcal/mol. Similarly, there are also some O⋯H interactions between the counteranion (OTf) of Yb(OTf)₃ and the chiral NAD(P)H model and 5a in the reduction process. In contrast, in the case of Yb(OTf)₃-assisted C=C bond reduction (Scheme 10b), the corresponding energy barrier (TS-LA-C=C, 8.9 kcal/mol) is obviously lower than that of C=N bonds (15.9 and 10.6 kcal/mol), mainly due to coordination interaction between Yb(OTf)₃ and double carbonyl groups of the substrate. Double functions of the NAD(P)H model and transfer catalyst play an important role in the formation of the cyclic transition state and enantioselective control.

CONCLUSIONS

In conclusion, we designed and synthesized a series of chiral and regenerable NAD(P)H with central, axial, and planar chiralities and applied them in biomimetic asymmetric reduction. In this process, hydrogen gas was the terminal reductant. Readily available and bench-stable achiral Brønsted acid or Lewis acid ytterbium/samarium triflate could be used as the transfer catalysts. This biomimetic asymmetric reduction features broad substrate scope, including various imines, electron-deficient alkenes, and heteroaromatic compounds

Scheme 11. Probable Reaction Mechanism, Optimized Stationary Points, and the Corresponding Free Energy in Solution Relative to Separated Reactants



with up to 99% yield and 99% ee. In addition, the detailed mechanism of chiral and regenerable NAD(P)H models enabling biomimetic asymmetric reduction has been investigated by a combination of experimental and theoretical studies. The isotope-labeling reactions indicated that the process suffered from the NAD(P)H models' regeneration under hydrogen gas, and then, the hydride transferred to the unsaturated bond, similar to the coenzyme NAD(P)H-mediated redox reaction process. Furthermore, density functional theory (DFT) calculations revealed the detailed transition state for the corresponding transfer catalyst and showed that the excellent enantioselectivity in the reaction resulted from the diastereotopic transfer of the hydrogen atom. The above mechanistic study may provide some useful hints for the design of a biomimetic catalytic system and extend the scope of chiral and regenerable NAD(P)H models enabling biomimetic asymmetric reduction.

EXPERIMENTAL SECTION

General. Unless otherwise noted, all reactions were carried out under an atmosphere of nitrogen using the standard Schlenk techniques. Commercially available reagents were used without further purification. Solvents were treated prior to use according to the standard methods. ^1H NMR and ^{13}C NMR spectra were recorded at 400 and 100 MHz with a Bruker spectrometer. ^{19}F NMR spectra were recorded at 376 MHz with a Bruker spectrometer. Chemical shifts are reported in parts per million (ppm) using tetramethylsilane as the internal standard when using CDCl_3 as the solvent for ^1H NMR spectra. The following abbreviations were used to symbolize the multiplicities: s, singlet; d, doublet; t, triplet; q, quartet; m, multiplet; br, broad. Flash column chromatography was performed on silica gel (200–300 mesh). All reactions were monitored by thin-layer chromatography (TLC) analysis. Optical rotations were measured by the polarimeter. Enantiomeric excess was determined by HPLC analysis using the chiral column described below in detail. The heat source for all heating reactions is an oil bath. High-resolution mass spectrometry (HRMS) was measured on an electrospray ionization (ESI) apparatus using time-of-flight (TOF) mass spectrometry.

Procedures for the Synthesis of NAD(P)H Models with Central Chirality. Under a nitrogen atmosphere, 6-methylphenanthridine (0.386 g, 2.0 mmol) was dissolved in ether (10 mL), followed by dropwise addition of *n*-butyllithium (1.6 M solution in hexanes) (1.40 mL, 2.2 mmol) at 0 °C. The mixture was stirred for 5 min at 0 °C. Then, the reaction was stirred for 1 h at ambient temperature. To a solution of *D*-camphor (0.304 g, 2.0 mmol) in ether (5 mL) under nitrogen was added at 0 °C. Next, the reaction was stirred at ambient temperature. When TLC indicated that the reaction was finished, the mixture was cooled to 0 °C. The reaction was quenched with water (15 mL) and extracted with ether (10 mL \times 3). The combined organic layer was dried over anhydrous sodium sulfate. After filtration, the solvent was removed under reduced pressure, and the residue was purified by flash column chromatography to give the corresponding product **1a**.

1,7,7-Trimethyl-2-(phenanthridin-6-ylmethyl)bicyclo[2.2.1]heptan-2-ol (1a). 0.220 g, 32% yield, white solid, mp 123–124 °C, new compound, $R_f = 0.75$ (hexane/ethyl acetate 10/1), ^1H NMR (400 MHz, CDCl_3) δ 8.63 (d, $J = 7.8$ Hz, 1H), 8.52 (d, $J = 7.7$ Hz, 1H), 8.26 (d, $J = 8.0$ Hz, 1H), 8.06 (d, $J = 7.8$ Hz, 1H), 7.89–7.79 (m, 1H), 7.76–7.66 (m, 2H), 7.65–7.58 (m, 1H), 7.32 (s, 1H), 3.55 (s, 2H), 2.29 (d, $J = 12.9$ Hz, 1H), 1.85–1.70 (m, 2H), 1.69–1.57 (m, 1H), 1.55–1.43 (m, 2H), 1.27 (s, 3H), 1.19–1.08 (m, 1H), 0.89 (s, 3H), 0.85 (s, 3H). $^{13}\text{C}\{^1\text{H}\}$ NMR (100 MHz, CDCl_3) δ 161.0, 142.0, 132.9, 130.8, 129.4, 128.8, 127.6, 126.8, 126.0, 125.9, 123.4, 122.7, 122.0, 81.0, 52.9, 49.4, 47.9, 45.4, 40.0, 30.9, 27.3, 21.8, 21.2, 11.5. HRMS (ESI-TOF) m/z calcd for $\text{C}_{24}\text{H}_{28}\text{NO}$ [$\text{M} + \text{H}$] $^+$ 346.2165, found: 346.2165.

Procedures for the Synthesis of the NAD(P)H Model 1b with Axial Chirality. Under a nitrogen atmosphere, a mixture of 2-chloro-1-iodo-3-methylbenzene (7.94 g, 32 mmol), 2-bromobenzylamine (6.44 g, 35 mmol), cesium carbonate (21.52 g, 66 mmol), triphenylphosphine (0.82 g, 3.1 mmol), palladium diacetate (1.10 g, 4.5 mmol), and norbornene (1.48 g, 16 mmol) in *N,N*-dimethylformamide (DMF, 120 mL) was stirred for 24 h at 160 °C. When TLC indicated that the reaction was finished, the mixture was cooled to ambient temperature and extracted with ethyl acetate (30 mL \times 3). Then, the combined organic layer was dried over anhydrous sodium sulfate and concentrated in vacuo. The crude product was afforded by flash column chromatography.

Under a nitrogen atmosphere, a mixture of potassium *tert*-butoxide (59 mg, 0.53 mmol) and Pd-Cat (5 mg, 0.007 mmol) in 1,4-dioxane (2 mL) was stirred for 10 min. After naphthalen-1-yl-boronic acid (90 mg, 0.53 mmol) was added and stirred for 20 min, the above crude compound (80 mg, 0.38 mmol) was added and stirred at 100 °C for 16 h. The mixture was cooled to ambient temperature and extracted with ethyl acetate (20 mL \times 3). Then, the combined organic layer was dried over anhydrous sodium sulfate and concentrated in vacuo. The solid obtained was purified by flash column chromatography to achieve the product (\pm)-**1b** (white solid 52 mg, 20% yield for two

steps). mp = 136–137 °C, $R_f = 0.40$ (hexane/ethyl acetate 10/1). ^1H NMR (400 MHz, CDCl_3) δ 9.08 (s, 1H), 8.61 (dd, $J = 19.1, 8.4$ Hz, 2H), 7.98–7.88 (m, 3H), 7.86–7.79 (m, 1H), 7.70–7.60 (m, 3H), 7.45–7.39 (m, 2H), 7.28–7.17 (m, 2H), 2.15 (s, 3H); $^{13}\text{C}\{^1\text{H}\}$ NMR (100 MHz, CDCl_3) δ 153.3, 143.9, 139.2, 138.2, 137.9, 133.8, 132.7, 132.7, 130.8, 129.3, 128.7, 128.4, 127.6, 127.4, 127.2, 126.1, 125.9, 125.8, 125.7, 125.6, 122.1, 121.8, 121.6, 20.8. HRMS (ESI-TOF) m/z calcd for $\text{C}_{24}\text{H}_{18}\text{N}$ [$\text{M} + \text{H}$] $^+$ 320.1434, found: 320.1438.

The compound (\pm)-**1b** (634 mg, 2 mmol) was dissolved in acetone (8 mL) with heating to 40 °C. (+)-Di-*p*-methoxybenzoyl-*D*-tartaric acid (*D*-DMTA, 573 mg, 1.2 mmol) in acetone (6 mL) was added, and the mixture was stirred for 20 min. Then, 50 mL of hexane was added slowly. After stirring for 5 min, the mixture was cooled to ambient temperature. The crystals were filtered, washed with cold hexane three times, and dried to afford the solid diastereoisomeric salt. Workup of the diastereoisomeric salt was as follows. The crystal was added to sodium hydroxide aqueous solution and stirred for 30 min. The mixture was extracted with dichloromethane. Then, the combined organic phase was dried over anhydrous sodium sulfate and the solvent was removed in vacuo to afford the product. Repeating this operation three times gave the chiral compound (*R*)-(+)-**1b**. 78 mg, 12% yield, new compound, $[\alpha]_{\text{D}}^{20} = +76.36$ (*c* 0.66, CHCl_3), 94% ee HPLC (OD-H, elute: *n*-hexane/*i*-PrOH = 97/3, detector: 220 nm, 30 °C, flow rate: 0.7 mL/min), $t_1 = 15.0$ min (major), $t_2 = 18.0$ min.

Procedures for the Synthesis of the NAD(P)H Model 1c with Axial Chirality. Under a nitrogen atmosphere, a mixture of 4-bromophenanthridine (0.994 g, 3.9 mmol), (2-methylnaphthalen-1-yl)boronic acid (1.040 g, 5.6 mmol), potassium carbonate (0.953 g, 6.8 mmol), and tetrakis(triphenylphosphine)palladium (0.199 g, 0.17 mmol) in dimethoxyethane/water (50/25 mL) was stirred at 95 °C for 24 h. The mixture was cooled to ambient temperature and extracted with ethyl acetate (30 mL \times 3). Then, the combined organic layer was dried over anhydrous sodium sulfate and concentrated in vacuo. The crude product obtained was purified by flash column chromatography using hexanes and ethyl acetate as the eluent to achieve the racemic product (\pm)-**1c** (white solid, 1.20 g, 97% yield). mp = 156–157 °C, $R_f = 0.40$ (hexane/ethyl acetate 10/1). ^1H NMR (400 MHz, CDCl_3) δ 9.15 (s, 1H), 8.73 (d, $J = 8.3$ Hz, 2H), 7.99 (d, $J = 7.9$ Hz, 1H), 7.97–7.85 (m, 3H), 7.81 (t, $J = 7.7$ Hz, 1H), 7.71 (t, $J = 7.5$ Hz, 1H), 7.62 (d, $J = 7.1$ Hz, 1H), 7.51 (d, $J = 8.4$ Hz, 1H), 7.36 (dd, $J = 10.6, 3.9$ Hz, 1H), 7.23–7.14 (m, 2H), 2.14 (s, 3H); $^{13}\text{C}\{^1\text{H}\}$ NMR (100 MHz, CDCl_3) δ 153.5, 143.4, 140.0, 137.6, 134.0, 133.4, 132.8, 132.1, 131.1, 130.9, 128.8, 128.7, 127.9, 127.6, 126.8, 126.3, 125.7, 124.6, 124.5, 122.1, 122.0, 20.9. HRMS (ESI-TOF) m/z calcd for $\text{C}_{24}\text{H}_{18}\text{N}$ [$\text{M} + \text{H}$] $^+$ 320.1434, found: 320.1436.

The compound (\pm)-**1c** (2.17 g, 6.8 mmol) was dissolved in acetone (6 mL) with heating to 40 °C. (+)-Di-*p*-methoxybenzoyl-*D*-tartaric acid (*D*-DMTA, 1.80 g, 3.7 mmol) in acetone (3 mL) was added, and the mixture was stirred for 20 min. Then, 20 mL of hexane was added slowly. After stirring for 5 min, the mixture was cooled to ambient temperature. The crystals were filtered, washed with cold hexane three times, and dried to afford the solid diastereoisomeric salt. Workup of the diastereoisomeric salt was as follows. The crystal was added to sodium hydroxide aqueous solution and stirred for 30 min. The mixture was extracted with dichloromethane. Then, the combined organic phase was dried and the solvent was removed in vacuo to afford the product. Repeating this operation three times gave the chiral compound (*R*)-(–)-**1c**. 981 mg, 45% yield, $[\alpha]_{\text{D}}^{20} = -27.24$ (*c* 0.58, CHCl_3), 99% ee HPLC (OD-H, elute: *n*-hexane/*i*-PrOH = 99/1, detector: 254 nm, 30 °C, flow rate: 0.4 mL/min), $t_1 = 21.7$ min (major), $t_2 = 25.9$ min.

Procedures for the Synthesis of the NAD(P)H Model 1d with Axial Chirality. Under a nitrogen atmosphere, a mixture of 2-amino-6-bromobenzaldehyde (4.10 g, 20 mmol), (2-nitrophenyl)boronic acid (3.76 g, 23 mmol), potassium carbonate (5.76 g, 41 mmol), and tetrakis(triphenylphosphine)palladium (2.13 g, 1.84 mmol) in dimethyl ether (DME)/water (35/20 mL) was stirred at 95 °C for 48 h. The mixture was cooled to ambient temperature and extracted with ethyl acetate (30 mL \times 3). Then, the combined organic layer was dried over anhydrous sodium sulfate and concentrated in

vacuo. The crude product was afforded by flash column chromatography (gray oil, 2.17 g, 44% yield). $R_f = 0.60$ (hexane/ethyl acetate 2/1). $^1\text{H NMR}$ (400 MHz, CDCl_3) δ 9.65 (s, 1H), 8.01 (dd, $J = 8.1, 1.2$ Hz, 1H), 7.66–7.61 (m, 1H), 7.58–7.53 (m, 1H), 7.39 (dd, $J = 7.5, 1.5$ Hz, 1H), 7.29–7.24 (m, 1H), 6.69 (d, $J = 8.4$ Hz, 1H), 6.55–6.35 (m, 1H; brs, 2H); $^{13}\text{C}\{^1\text{H}\}$ NMR (100 MHz, CDCl_3) δ 192.6, 150.8, 149.2, 143.3, 134.6, 134.0, 132.7, 132.3, 129.0, 124.2, 117.2, 117.0, 116.1.

A mixture of the above crude product (1.91 g, 7.9 mmol) and iron powder (1.76 g, 31.6 mmol) in ethanol (10 mL) was stirred at 75 °C, and conc. HCl (5.30 mL) was added slowly. When TLC indicated that the reaction was finished, the mixture was cooled to ambient temperature and saturated sodium hydrogen carbonate solution was added. The mixture was extracted with dichloromethane (30 mL \times 3). Then, the combined organic layer was dried over anhydrous sodium sulfate and concentrated in vacuo. The crude product was afforded by flash column chromatography (orange solid, 1.22 g, 80% yield).

To a solution of the above product (615 mg, 3.15 mmol) in water (10 mL) was added conc. HCl (4.2 mL) and stirred for 5 min. A solution of sodium nitrite (283 mg, 4.10 mmol) in H_2O (8 mL) was added slowly. After stirring for 3 h at ambient temperature, a solution of potassium iodide (837 mg, 5.04 mmol) in water (10 mL) was added to the reaction. After stirring for 3 h at 60 °C, the mixture was cooled to ambient temperature and saturated sodium hydrogen carbonate solution was added. The mixture was extracted with dichloromethane (30 mL \times 3). Then, the combined organic layer was dried over anhydrous sodium sulfate and concentrated in vacuo. The crude product was afforded by flash column chromatography (purple solid, 0.717 g, 75% yield). $^1\text{H NMR}$ (400 MHz, CDCl_3) δ 9.48 (s, 1H), 8.59–8.48 (m, 2H), 8.23–8.16 (m, 2H), 7.79–7.74 (m, 1H), 7.71–7.66 (m, 1H), 7.51–7.45 (m, 1H); ^{13}C NMR (100 MHz, CDCl_3) δ 157.1, 144.6, 139.0, 134.3, 131.7, 130.3, 129.4, 127.6, 126.1, 122.8, 122.5, 122.0, 99.6.

Under a nitrogen atmosphere, a mixture of the above crude product (516 mg, 1.7 mmol), potassium carbonate (467 mg, 3.4 mmol), (2-methylnaphthalen-1-yl)-boronic acid (629 mg, 3.4 mmol), and tetrakis(triphenylphosphine)palladium (195 mg, 0.17 mmol) in DME/water (30/15 mL) was stirred at 95 °C for 24 h. The mixture was cooled to ambient temperature and extracted with ethyl acetate (30 mL \times 3). Then, the combined organic layer was dried over anhydrous sodium sulfate and concentrated in vacuo. The product (\pm)-**1d** was afforded by flash column chromatography (white solid, 186 mg, 34% yield). mp = 165–166 °C, $R_f = 0.40$ (hexane/ethyl acetate 10/1). $^1\text{H NMR}$ (400 MHz, CDCl_3) δ 8.79–8.67 (m, 3H), 8.19–8.10 (m, 1H), 8.04–7.95 (m, 1H), 7.94–7.87 (m, 2H), 7.78–7.68 (m, 2H), 7.58 (d, $J = 7.1$ Hz, 1H), 7.51 (d, $J = 8.5$ Hz, 1H), 7.41 (t, $J = 7.5$ Hz, 1H), 7.28–7.19 (m, 1H), 7.10 (d, $J = 8.5$ Hz, 1H), 2.14 (s, 3H); $^{13}\text{C}\{^1\text{H}\}$ NMR (100 MHz, CDCl_3) δ 152.0, 144.4, 139.6, 134.6, 134.1, 133.5, 133.0, 132.0, 130.8, 130.2, 129.7, 128.8, 128.5, 128.3, 128.0, 127.2, 126.3, 125.9, 125.2, 125.1, 124.2, 122.4, 121.4, 20.7. HRMS (ESI-TOF) m/z calcd for $\text{C}_{24}\text{H}_{18}\text{N}$ $[\text{M} + \text{H}]^+$ 320.1434, found: 320.1438.

The compound (\pm)-**1d** (306 mg, 1 mmol) was dissolved in acetone (3 mL) with heating to 40 °C. (+)-Di-*p*-methoxybenzoyl-*D*-tartaric acid (*D*-DMTA, 254 mg, 0.5 mmol) in acetone (1 mL) was added, and the mixture was stirred for 20 min. Then, 20 mL of hexane was added slowly. After stirring for 5 min, the mixture was cooled to ambient temperature. The crystals were filtered, washed with cold hexane three times, and dried to afford the solid diastereoisomeric salt. Workup of the diastereoisomeric salt was as follows. The crystal was added to sodium hydroxide aqueous solution and stirred for 30 min. The mixture was extracted with dichloromethane. Then, the combined organic phase was dried and the solvent was removed in vacuo to afford the product. Repeating this operation three times gave the chiral (*R*)-(-)-**1d**. 39 mg, 13% yield, $[\alpha]_{\text{D}}^{20} = +11.33$ (*c* 0.15, CHCl_3), 92% ee HPLC (OD-H, elute: *n*-hexane/*i*-PrOH = 95/5, detector: 254 nm, 30 °C, flow rate: 0.5 mL/min), $t_1 = 15.2$ min (major), $t_2 = 17.9$ min.

Procedures for the Synthesis of the NAD(P)H Model 1e with Axial Chirality. Under a nitrogen atmosphere, a mixture of 2,6-dibromobenzaldehyde (729 mg, 2.77 mmol), (2-nitrophenyl)boronic acid (507 mg, 3.05 mmol), potassium carbonate (763 mg, 5.54 mmol), and tetrakis(triphenylphosphine)palladium (96 mg, 0.08 mmol) in DME/water (15/8 mL) was stirred at 95 °C for 24 h. The mixture was cooled to ambient temperature and extracted with ethyl acetate (30 mL \times 3). Then, the combined organic layer was dried over anhydrous sodium sulfate and concentrated in vacuo. The crude product (118 mg, 14% yield) was afforded by flash column chromatography.

A mixture of the above crude product (118 mg, 0.4 mmol) and iron powder (65 mg, 1.2 mmol) in ethanol (10 mL) was stirred at 75 °C and conc. HCl (0.30 mL) was added. When TLC indicated that the reaction was finished, the mixture was cooled to ambient temperature and saturated sodium hydrogen carbonate solution was added. The mixture was extracted with dichloromethane (30 mL \times 3). Then, the combined organic layer was dried over anhydrous sodium sulfate and concentrated in vacuo. The crude product was afforded by flash column chromatography (39 mg, 39% yield).

Under a nitrogen atmosphere, a mixture of the above product (1.85 g, 7.2 mmol), (2-methoxynaphthalen-1-yl)boronic acid (1.88 g, 9.36 mmol), potassium carbonate (1.98 g, 14.4 mmol), and tetrakis(triphenylphosphine)palladium (414 mg, 0.36 mmol) in DME/water (40/20 mL) was stirred at 95 °C for 4 h. The mixture was cooled to ambient temperature and extracted with ethyl acetate (30 mL \times 3). Then, the combined organic layer was dried over anhydrous sodium sulfate and concentrated in vacuo. The product (\pm)-**1e** was afforded by flash column chromatography (2.40 g, 99% yield). White solid, mp = 155–156 °C, $R_f = 0.10$ (hexane/ethyl acetate 10/1). $^1\text{H NMR}$ (400 MHz, CDCl_3) δ 8.84 (s, 1H), 8.75–8.65 (m, 2H), 8.13 (d, $J = 7.8$ Hz, 1H), 8.06–7.93 (m, 2H), 7.88 (d, $J = 8.1$ Hz, 1H), 7.76–7.66 (m, 2H), 7.62 (d, $J = 7.2$ Hz, 1H), 7.44 (d, $J = 9.1$ Hz, 1H), 7.33 (t, $J = 7.4$ Hz, 1H), 7.28–7.22 (m, 1H), 7.20–7.16 (m, 1H), 3.76 (s, 3H); $^{13}\text{C}\{^1\text{H}\}$ NMR (100 MHz, CDCl_3) δ 154.6, 152.4, 144.4, 136.7, 134.2, 132.9, 130.6, 130.5, 130.3, 130.1, 129.0, 128.6, 128.1, 127.0, 126.9, 125.5, 125.0, 124.4, 123.8, 122.4, 121.4, 120.9, 113.1, 56.5. HRMS (ESI-TOF) m/z calcd for $\text{C}_{24}\text{H}_{18}\text{NO}$ $[\text{M} + \text{H}]^+$ 336.1383, found: 336.1389.

The compound (\pm)-**1e** (2.24 g, 6.7 mmol) was dissolved in acetone (40 mL) with heating to 40 °C. (+)-Di-*p*-methoxybenzoyl-*D*-tartaric acid (*D*-DMTA, 1.93 g, 4.0 mmol) in acetone (10 mL) was added, and the mixture was stirred for 20 min. The mixture was cooled to ambient temperature. The crystals were filtered, washed with cold hexane three times, and dried to afford the solid diastereoisomeric salt. Workup of the diastereoisomeric salt was as follows. The crystal was added to sodium hydroxide aqueous solution and stirred for 30 min. The mixture was extracted with dichloromethane. Then, the combined organic phase was dried over anhydrous sodium sulfate and the solvent was removed in vacuo to afford the product. Repeating this operation four times gave the chiral compound (*R*)-(+)-**1e**. 490 mg, 22% yield, $[\alpha]_{\text{D}}^{20} = +115.29$ (*c* 0.66, CHCl_3), 99% ee HPLC (OD-H, elute: *n*-hexane/*i*-PrOH = 96/4, detector: 220 nm, 30 °C, flow rate: 0.6 mL/min), $t_1 = 16.1$ min, $t_2 = 29.9$ min (major).

Brønsted Acid-Promoted Biomimetic Asymmetric Reduction. Synthesis of the Substrates. Quinoxalinones **3**,^{12b} benzoxazinones **5**,^{12b} benzoxazine **7**,^{12b} and alkylnyl ketimines **9**^{8b} could be conveniently prepared according to the known literature procedure. All compounds **3**, **5**, **7**, and **9** are known.

Procedures for Biomimetic Asymmetric Reduction of Quinoxalinones. A mixture of $[\text{Ru}(p\text{-cymene})\text{I}_2]_2$ (0.7 mg, 0.00075 mmol), diphenyl hydrogen phosphate **2a** (1.5 mg, 0.006 mmol), the NAD(P)H model (*R*)-**1g** (4.5 mg, 0.015 mmol), and quinoxalinone **3** (0.15 mmol) in chloroform (3 mL) was stirred at room temperature for 5 min in a glovebox, and then, the mixture was transferred to an autoclave. Hydrogenation was performed at 40 °C under hydrogen gas (500 psi) for 48 h. After careful release of the hydrogen gas, the autoclave was opened and the reaction mixture was directly purified

by column chromatography on silica gel using hexane and ethyl acetate as the eluent to give the chiral reductive products 4.

(-)-(R)-1-Methyl-3-phenyl-3,4-dihydroquinoxalin-2(1H)-one (**4a**). 23 mg for 0.1 mmol, 96% yield, white solid, known compound, $R_f = 0.41$ (hexane/ethyl acetate 5/1), 98% ee, $[\alpha]_D^{20} = -134.86$ (c 0.39, CHCl₃), [lit.:^{12b} $[\alpha]_D^{20} = +153.0$ (c 0.4, CHCl₃) for 92% ee]; ¹H NMR (400 MHz, CDCl₃) δ 7.40–7.35 (m, 2H), 7.33–7.26 (m, 3H), 6.97–6.91 (m, 2H), 6.88–6.83 (m, 1H), 6.73 (dd, $J = 7.6, 1.2$ Hz, 1H), 5.04 (s, 1H), 4.36 (brs, 1H), 3.37 (s, 3H); ¹³C{¹H} NMR (100 MHz, CDCl₃) δ 166.3, 139.3, 134.7, 128.9, 128.5, 128.5, 127.3, 124.0, 119.7, 115.0, 114.2, 61.0, 29.4. HPLC (AD-H, elute: *n*-hexane/*i*-PrOH = 80/20, detector: 230 nm, 30 °C, flow rate: 1.0 mL/min), $t_1 = 12.2$ min, $t_2 = 15.6$ min (major).

(-)-(R)-1-Methyl-3-(*p*-tolyl)-3,4-dihydroquinoxalin-2(1H)-one (**4b**). 36 mg, 95% yield, white solid, known compound, $R_f = 0.56$ (hexane/ethyl acetate 5/1), 98% ee, $[\alpha]_D^{20} = -127.63$ (c 0.72, CHCl₃), [lit.:^{12b} $[\alpha]_D^{20} = +106.2$ (c 0.4, CHCl₃) for 89% ee]; ¹H NMR (400 MHz, CDCl₃) δ 7.27 (d, $J = 8.0$ Hz, 2H), 7.13 (d, $J = 8.0$ Hz, 2H), 6.99–6.92 (m, 2H), 6.90–6.84 (m, 1H), 6.74 (dd, $J = 7.6, 0.9$ Hz, 1H), 5.01 (s, 1H), 4.38 (brs, 1H), 3.39 (s, 3H), 2.33 (s, 3H); ¹³C{¹H} NMR (100 MHz, CDCl₃) δ 166.4, 138.2, 136.3, 134.8, 129.6, 128.6, 127.2, 123.9, 119.6, 114.9, 114.2, 60.8, 29.4, 21.3. HPLC (AD-H, elute: *n*-hexane/*i*-PrOH = 80/20, detector: 230 nm, 30 °C, flow rate: 1.0 mL/min), $t_1 = 11.2$ min, $t_2 = 14.9$ min (major).

(-)-(R)-3-(4-Methoxyphenyl)-1-methyl-3,4-dihydroquinoxalin-2(1H)-one (**4c**). 38 mg, 95% yield, white solid, known compound, $R_f = 0.50$ (hexane/ethyl acetate 5/1), 98% ee, $[\alpha]_D^{20} = -138.15$ (c 0.76, CHCl₃), [lit.:^{12b} $[\alpha]_D^{20} = +120.9$ (c 0.4, CHCl₃) for 90% ee]; ¹H NMR (400 MHz, CDCl₃) δ 7.30 (d, $J = 8.7$ Hz, 2H), 6.99–6.92 (m, 2H), 6.91–6.82 (m, 3H), 6.76–6.71 (m, 1H), 5.00 (s, 1H), 4.32 (brs, 1H), 3.78 (s, 3H), 3.40 (s, 3H); ¹³C{¹H} NMR (100 MHz, CDCl₃) δ 165.6, 158.8, 133.8, 130.5, 127.6, 122.9, 118.7, 114.0, 113.3, 113.2, 59.6, 54.5, 28.4. HPLC (AD-H, elute: *n*-hexane/*i*-PrOH = 80/20, detector: 230 nm, 30 °C, flow rate: 1.0 mL/min), $t_1 = 16.7$ min, $t_2 = 19.7$ min (major).

(-)-(R)-3-(4-Bromophenyl)-1-methyl-3,4-dihydroquinoxalin-2(1H)-one (**4d**). 46 mg, 97% yield, white solid, known compound, $R_f = 0.60$ (hexane/ethyl acetate 5/1), 97% ee, $[\alpha]_D^{20} = -140.32$ (c 0.92, CHCl₃), [lit.:^{12b} $[\alpha]_D^{20} = +122.1$ (c 0.4, CHCl₃) for 94% ee]; ¹H NMR (400 MHz, CDCl₃) δ 7.44 (d, $J = 8.4$ Hz, 2H), 7.31–7.24 (m, 2H), 7.01–6.85 (m, 3H), 6.79–6.73 (m, 1H), 5.01 (s, 1H), 4.37 (brs, 1H), 3.38 (s, 3H); ¹³C{¹H} NMR (100 MHz, CDCl₃) δ 164.8, 137.1, 133.4, 131.0, 128.1, 127.4, 123.1, 121.6, 119.0, 114.1, 113.3, 59.5, 28.5. HPLC (OD-H, elute: *n*-hexane/*i*-PrOH = 80/20, detector: 230 nm, 30 °C, flow rate: 1.0 mL/min), $t_1 = 10.4$ min (major), $t_2 = 16.5$ min.

(-)-(R)-3-(3-Fluorophenyl)-1-methyl-3,4-dihydroquinoxalin-2(1H)-one (**4e**). 37 mg, 96% yield, white solid, known compound, $R_f = 0.45$ (hexane/ethyl acetate 5/1), 99% ee, $[\alpha]_D^{20} = -161.75$ (c 0.74, CHCl₃), [lit.:^{12b} $[\alpha]_D^{20} = +121.8$ (c 0.4, CHCl₃) for 91% ee]; ¹H NMR (400 MHz, CDCl₃) δ 7.34–7.25 (m, 1H), 7.18 (d, $J = 7.8$ Hz, 1H), 7.12 (d, $J = 9.7$ Hz, 1H), 7.02–6.93 (m, 3H), 6.91–6.86 (m, 1H), 6.77 (d, $J = 7.8$ Hz, 1H), 5.06 (s, 1H), 4.44 (brs, 1H), 3.39 (s, 3H); ¹³C{¹H} NMR (100 MHz, CDCl₃) δ 165.7, 163.8 (d, ¹ $J_{F-C} = 245.0$ Hz), 141.7 (d, ³ $J_{F-C} = 6.3$ Hz), 134.3, 130.4 (d, ³ $J_{F-C} = 7.8$ Hz), 128.4, 124.1, 123.0, 120.0, 115.4 (d, ² $J_{F-C} = 21.1$ Hz), 115.1, 114.4 (d, ² $J_{F-C} = 21.1$ Hz), 114.3, 60.5, 29.5; ¹⁹F{¹H} NMR (376 MHz, CDCl₃) δ -112.17. HPLC (AD-H, elute: *n*-hexane/*i*-PrOH = 85/15, detector: 230 nm, 30 °C, flow rate: 1.0 mL/min), $t_1 = 13.3$ min, $t_2 = 17.2$ min (major).

(+)-(R)-3-(2-Methoxyphenyl)-1-methyl-3,4-dihydroquinoxalin-2(1H)-one (**4f**). 38 mg, 95% yield, white solid, known compound, $R_f = 0.40$ (hexane/ethyl acetate 5/1), 98% ee, $[\alpha]_D^{20} = +107.36$ (c 0.76, CHCl₃), [lit.:^{12b} $[\alpha]_D^{20} = -168.4$ (c 0.4, CHCl₃) for 74% ee]; ¹H NMR (400 MHz, CDCl₃) δ 7.29–7.22 (m, 1H), 7.03 (dd, $J = 7.5, 1.3$ Hz, 1H), 6.97 (dd, $J = 7.6, 1.4$ Hz, 1H), 6.92–6.80 (m, 4H), 6.60 (dd, $J = 7.3, 1.5$ Hz, 1H), 5.46 (s, 1H), 4.52 (brs, 1H), 3.87 (s, 3H), 3.50 (s, 3H); ¹³C{¹H} NMR (100 MHz, CDCl₃) δ 166.6, 157.4, 134.9, 129.6, 129.0, 127.7, 126.9, 123.8, 120.9, 119.6, 114.8, 114.6, 111.1, 56.0, 55.8, 29.3. HPLC (OD-H, elute: *n*-hexane/*i*-PrOH = 80/20,

detector: 230 nm, 30 °C, flow rate: 1.0 mL/min), $t_1 = 13.6$ min, $t_2 = 16.4$ min (major).

(-)-(R)-1-Benzyl-3-phenyl-3,4-dihydroquinoxalin-2(1H)-one (**4g**). 44 mg, 93% yield, yellow solid, known compound, $R_f = 0.45$ (hexane/ethyl acetate 5/1), 99% ee, $[\alpha]_D^{20} = -150.33$ (c 0.88, CHCl₃), [lit.:^{12b} $[\alpha]_D^{20} = +79.0$ (c 0.2, CHCl₃) for 91% ee]; ¹H NMR (400 MHz, CDCl₃) δ 7.48–7.44 (m, 2H), 7.38–7.32 (m, 3H), 7.30–7.22 (m, 3H), 7.18 (d, $J = 7.3$ Hz, 2H), 6.96–6.92 (m, 1H), 6.87–6.83 (m, 1H), 6.78–6.71 (m, 2H), 5.31 (d, $J = 16.1$ Hz, 1H), 5.18 (s, 1H), 5.10 (d, $J = 16.1$ Hz, 1H), 4.50 (brs, 1H); ¹³C{¹H} NMR (100 MHz, CDCl₃) δ 166.4, 139.1, 136.8, 134.9, 129.0, 128.9, 128.6, 127.7, 127.3, 126.6, 124.1, 119.7, 115.8, 114.4, 61.0, 46.0. HPLC (AD-H, elute: *n*-hexane/*i*-PrOH = 80/20, detector: 230 nm, 30 °C, flow rate: 1.0 mL/min), $t_1 = 18.4$ min, $t_2 = 20.2$ min (major).

(-)-(R)-1-Allyl-3-phenyl-3,4-dihydroquinoxalin-2(1H)-one (**4h**). 37 mg, 93% yield, yellow solid, known compound, $R_f = 0.45$ (hexane/ethyl acetate 5/1), 99% ee, $[\alpha]_D^{20} = -112.29$ (c 0.74, CHCl₃), [lit.:^{12b} $[\alpha]_D^{20} = +93.0$ (c 0.2, CHCl₃) for 91% ee]; ¹H NMR (400 MHz, CDCl₃) δ 7.43–7.38 (m, 2H), 7.36–7.29 (m, 3H), 6.98–6.91 (m, 2H), 6.87–6.81 (m, 1H), 6.77 (d, $J = 7.7$ Hz, 1H), 5.93–5.83 (m, 1H), 5.19–5.07 (m, 2H; s, 1H), 4.72–4.63 (m, 1H), 4.55–4.47 (m, 1H), 4.42 (brs, 1H); ¹³C{¹H} NMR (100 MHz, CDCl₃) δ 165.9, 139.1, 134.8, 132.2, 128.9, 128.5, 127.7, 127.2, 124.0, 119.8, 116.9, 115.6, 114.4, 61.0, 44.9. HPLC (AD-H, elute: *n*-hexane/*i*-PrOH = 80/20, detector: 230 nm, 30 °C, flow rate: 1.0 mL/min), $t_1 = 10.6$ min, $t_2 = 16.3$ min (major).

(-)-(R)-1,3-Dimethyl-3,4-dihydroquinoxalin-2(1H)-one (**4i**). 25 mg, 94% yield, yellow oil, known compound, $R_f = 0.41$ (hexane/ethyl acetate 5/1), 96% ee, $[\alpha]_D^{20} = -367.57$ (c 0.50, CHCl₃), [lit.:^{12b} $[\alpha]_D^{20} = +65.0$ (c 0.2, CHCl₃) for 8% ee]; ¹H NMR (400 MHz, CDCl₃) δ 6.95–6.90 (m, 2H), 6.89–6.83 (m, 1H), 6.74–6.69 (m, 1H), 4.02–3.92 (m, 1H; brs, 1H), 3.36 (s, 3H), 1.44 (d, $J = 6.6$ Hz, 3H); ¹³C{¹H} NMR (100 MHz, CDCl₃) δ 168.6, 135.2, 129.3, 123.6, 119.8, 114.8, 114.4, 52.4, 29.2, 18.0. HPLC (AD-H, elute: *n*-hexane/*i*-PrOH = 85/15, detector: 230 nm, 30 °C, flow rate: 1.0 mL/min), $t_1 = 7.7$ min, $t_2 = 8.2$ min (major).

(-)-(R)-3-Ethyl-1-methyl-3,4-dihydroquinoxalin-2(1H)-one (**4j**). 28 mg, 98% yield, colorless oil, known compound,²³ $R_f = 0.50$ (hexane/ethyl acetate 5/1), 97% ee, $[\alpha]_D^{20} = -59.82$ (c 0.56, CHCl₃), ¹H NMR (400 MHz, CDCl₃) δ 6.95–6.88 (m, 2H), 6.87–6.80 (m, 1H), 6.71 (d, $J = 7.8$ Hz, 1H), 4.06 (brs, 1H), 3.84–3.78 (m, 1H), 3.36 (s, 3H), 1.91–1.79 (m, 1H), 1.78–1.67 (m, 1H), 1.01 (t, $J = 7.5$ Hz, 3H); ¹³C{¹H} NMR (100 MHz, CDCl₃) δ 168.0, 134.8, 129.1, 123.7, 119.6, 114.7, 114.4, 58.0, 29.2, 25.0, 10.0. HPLC (AD-H, elute: *n*-hexane/*i*-PrOH = 85/15, detector: 230 nm, 30 °C, flow rate: 1.0 mL/min), $t_1 = 7.8$ min, $t_2 = 9.1$ min (major).

(-)-(R)-3-Isopropyl-1-methyl-3,4-dihydroquinoxalin-2(1H)-one (**4k**). 28 mg, 92% yield, yellow oil, new compound, $R_f = 0.52$ (hexane/ethyl acetate 5/1), 99% ee, $[\alpha]_D^{20} = -18.03$ (c 0.56, CHCl₃), ¹H NMR (400 MHz, CDCl₃) δ 6.94–6.86 (m, 2H), 6.83–6.77 (m, 1H), 6.71–6.66 (m, 1H), 4.10 (brs, 1H), 3.71–3.66 (m, 1H), 3.37 (s, 3H), 2.25–2.10 (m, 1H), 1.01 (d, $J = 7.0$ Hz, 3H), 0.93 (d, $J = 6.7$ Hz, 3H); ¹³C{¹H} NMR (100 MHz, CDCl₃) δ 167.1, 135.0, 128.7, 123.7, 119.2, 114.7, 113.9, 62.4, 30.6, 29.2, 19.3, 17.9. HPLC (AD-H, elute: *n*-hexane/*i*-PrOH = 85/15, detector: 230 nm, 30 °C, flow rate: 1.0 mL/min), $t_1 = 7.6$ min, $t_2 = 9.4$ min (major). HRMS (ESI-TOF) m/z calcd for C₁₂H₁₇N₂O [M + H]⁺ 205.1335, found: 205.1339.

(-)-(R)-3-Butyl-1-methyl-3,4-dihydroquinoxalin-2(1H)-one (**4l**). 32 mg, 98% yield, yellow oil, new compound, $R_f = 0.52$ (hexane/ethyl acetate 5/1), 96% ee, $[\alpha]_D^{20} = -35.15$ (c 0.64, CHCl₃), ¹H NMR (400 MHz, CDCl₃) δ 6.95–6.88 (m, 2H), 6.87–6.81 (m, 1H), 6.71 (d, $J = 7.8$ Hz, 1H), 4.03 (brs, 1H), 3.88–3.83 (m, 1H), 3.36 (s, 3H), 1.86–1.76 (m, 1H), 1.73–1.61 (m, 1H), 1.47–1.28 (m, 4H), 0.91 (t, $J = 7.0$ Hz, 3H); ¹³C{¹H} NMR (100 MHz, CDCl₃) δ 168.2, 134.8, 129.1, 123.7, 119.6, 114.7, 114.5, 56.9, 31.5, 29.2, 27.8, 22.7, 14.2. HPLC (AD-H, elute: *n*-hexane/*i*-PrOH, detector: 230 nm, 30 °C, flow rate: 1.0 mL/min), $t_1 = 7.7$ min, $t_2 = 9.4$ min (major). HRMS (ESI-TOF) m/z calcd for C₁₃H₁₉N₂O [M + H]⁺ 219.1492, found: 219.1493.

Procedures for Biomimetic Asymmetric Reduction of Benzoxazinones. A mixture of [Ru(*p*-cymene)₂]₂ (0.7 mg, 0.00075 mmol), bis(4-nitrophenyl)hydrogen phosphate **2b** (2.6 mg, 0.0075 mmol), the NAD(P)H model (*R*)-**1f** (4.3 mg, 0.015 mmol), and benzoxazinone **5** (0.15 mmol) in chloroform (3 mL) was stirred at room temperature for 5 min in a glovebox, and then, the mixture was transferred to an autoclave. Hydrogenation was performed at 50 °C under hydrogen gas (500 psi) for 48 h. After careful release of hydrogen gas, the autoclave was opened and the reaction mixture was directly purified by column chromatography on silica gel using hexane and ethyl acetate as the eluent to give the corresponding chiral reductive products **6**. The enantiomeric excesses were determined by chiral HPLC.

(-)-(*R*)-3-Phenyl-3,4-dihydro-2H-benzo[b][1,4]oxazin-2-one (**6a**). 32 mg, 94% yield, white solid, known compound, *R*_f = 0.50 (hexane/ethyl acetate 5/1), 98% ee, [α]_D²⁰ = -134.92 (c 0.75, CHCl₃), [lit.:^{12b} [α]_D²⁰ = +106.5 (c 0.4, CHCl₃) for 97% ee]; ¹H NMR (400 MHz, CDCl₃) δ 7.42–7.31 (m, 5H), 7.05–6.97 (m, 2H), 6.88–6.82 (m, 1H), 6.81–6.77 (m, 1H), 5.03 (d, *J* = 1.7 Hz, 1H), 4.28 (brs, 1H); ¹³C{¹H} NMR (100 MHz, CDCl₃) δ 165.3, 140.9, 136.4, 132.4, 129.0, 127.5, 125.2, 120.4, 117.0, 114.9, 59.3. HPLC (OD-H, elute: *n*-hexane/*i*-PrOH = 70/30, detector: 230 nm, 30 °C, flow rate: 0.7 mL/min), *t*₁ = 11.9 min (major), *t*₂ = 15.8 min.

(-)-(*R*)-3-(*p*-Tolyl)-3,4-dihydro-2H-benzo[b][1,4]oxazin-2-one (**6b**). 34 mg, 94% yield, white solid, known compound, *R*_f = 0.50 (hexane/ethyl acetate 5/1), 98% ee, [α]_D²⁰ = -127.20 (c 0.68, CHCl₃), [lit.:^{12b} [α]_D²⁰ = +85.0 (c 0.4, CHCl₃) for 86% ee]; ¹H NMR (400 MHz, CDCl₃) δ 7.26 (d, *J* = 8.1 Hz, 2H), 7.15 (d, *J* = 8.0 Hz, 2H), 7.04–6.97 (m, 2H), 6.87–6.81 (m, 1H), 6.78 (d, *J* = 7.8 Hz, 1H), 4.98 (d, *J* = 1.4 Hz, 1H), 4.24 (brs, 1H), 2.32 (s, 3H); ¹³C{¹H} NMR (100 MHz, CDCl₃) δ 165.5, 141.0, 138.9, 133.4, 132.5, 129.7, 127.4, 125.2, 120.3, 116.9, 114.9, 59.0, 21.2. HPLC (OD-H, elute: *n*-hexane/*i*-PrOH = 70/30, detector: 230 nm, 30 °C, flow rate: 0.7 mL/min), *t*₁ = 9.4 min (major), *t*₂ = 23.8 min.

(-)-(*R*)-3-(4-Methoxyphenyl)-3,4-dihydro-2H-benzo[b][1,4]oxazin-2-one (**6c**). 37 mg, 97% yield, white solid, known compound, *R*_f = 0.20 (hexane/ethyl acetate 10/1), 97% ee, [α]_D²⁰ = -98.91 (c 0.74, CHCl₃), [lit.:^{12b} [α]_D²⁰ = +69.0 (c 0.2, CHCl₃) for 80% ee]; ¹H NMR (400 MHz, CDCl₃) δ 7.29 (d, *J* = 8.6 Hz, 2H), 7.01 (t, *J* = 8.5 Hz, 2H), 6.92–6.81 (m, 3H), 6.78 (d, *J* = 7.8 Hz, 1H), 4.95 (d, *J* = 0.6 Hz, 1H), 4.26 (brs, 1H), 3.77 (s, 3H); ¹³C{¹H} NMR (100 MHz, CDCl₃) δ 165.6, 160.0, 141.0, 132.6, 128.8, 128.4, 125.2, 120.3, 116.9, 114.9, 114.4, 58.8, 55.3. HPLC (OD-H, elute: *n*-hexane/*i*-PrOH = 70/30, detector: 230 nm, 30 °C, flow rate: 0.7 mL/min), *t*₁ = 11.5 min (major), *t*₂ = 24.9 min.

(-)-(*R*)-3-(4-Fluorophenyl)-3,4-dihydro-2H-benzo[b][1,4]oxazin-2-one (**6d**). 34 mg, 94% yield, known compound, white solid, *R*_f = 0.40 (hexane/ethyl acetate 10/1), 97% ee, [α]_D²⁰ = -124.84 (c 0.68, CHCl₃), [lit.:^{12b} [α]_D²⁰ = +107.0 (c 0.2, CHCl₃) for 89% ee]; ¹H NMR (400 MHz, CDCl₃) δ 7.43–7.33 (m, 2H), 7.10–6.99 (m, 4H), 6.91–6.84 (m, 1H), 6.83–6.79 (m, 1H), 5.02 (d, *J* = 1.2 Hz, 1H), 4.27 (brs, 1H); ¹³C{¹H} NMR (100 MHz, CDCl₃) δ 165.2, 163.0 (d, ¹*J*_{F-C} = 246.6 Hz), 140.9, 132.3, 132.1 (d, ⁴*J*_{F-C} = 3.3 Hz), 129.4 (d, ³*J*_{F-C} = 8.3 Hz), 125.3, 120.6, 117.0, 116.0 (d, ²*J*_{F-C} = 21.7 Hz), 115.0, 58.7; ¹⁹F{¹H} NMR (376 MHz, CDCl₃) δ -112.46. HPLC (AD-H, elute: *n*-hexane/*i*-PrOH = 80/20, detector: 230 nm, 30 °C, flow rate: 0.8 mL/min), *t*₁ = 10.9 min, *t*₂ = 13.5 min (major).

(-)-(*R*)-3-(4-Chlorophenyl)-3,4-dihydro-2H-benzo[b][1,4]oxazin-2-one (**6e**). 38 mg, 97% yield, white solid, known compound, 93% ee, *R*_f = 0.40 (hexane/ethyl acetate 10/1), [α]_D²⁰ = -119.99 (c 0.76, CHCl₃), [lit.:^{12b} [α]_D²⁰ = +90.0 (c 0.2, CHCl₃) for 87% ee]; ¹H NMR (400 MHz, CDCl₃) δ 7.36–7.32 (s, 4H), 7.07–6.98 (m, 2H), 6.91–6.85 (m, 1H), 6.84–6.79 (m, 1H), 5.01 (d, *J* = 2.0 Hz, 1H), 4.28 (brs, 1H); ¹³C{¹H} NMR (100 MHz, CDCl₃) δ 164.9, 140.9, 135.0, 134.8, 132.1, 129.2, 128.9, 125.3, 120.7, 117.0, 115.0, 58.7. HPLC (AD-H, elute: *n*-hexane/*i*-PrOH = 80/20, detector: 230 nm, 30 °C, flow rate: 0.8 mL/min), *t*₁ = 11.4 min, *t*₂ = 13.2 min (major).

(-)-(*R*)-3-(4-Bromophenyl)-3,4-dihydro-2H-benzo[b][1,4]oxazin-2-one (**6f**). 43 mg, 96% yield, white solid, known compound, *R*_f = 0.20 (hexane/ethyl acetate 10/1), 92% ee, [α]_D²⁰ = -108.83 (c 0.86,

CHCl₃), [lit.:^{12b} [α]_D²⁰ = +83.0 (c 0.2, CHCl₃) for 90% ee]; ¹H NMR (400 MHz, CDCl₃) δ 7.49 (d, *J* = 8.4 Hz, 2H), 7.28 (d, *J* = 8.4 Hz, 2H), 7.06–7.00 (m, 2H), 6.91–6.85 (m, 1H), 6.84–6.80 (m, 1H), 5.01 (d, *J* = 1.7 Hz, 1H), 4.26 (brs, 1H); ¹³C{¹H} NMR (100 MHz, CDCl₃) δ 164.8, 140.9, 135.3, 132.2, 132.1, 129.2, 125.3, 123.2, 120.7, 117.1, 115.0, 58.8. HPLC (AD-H, elute: *n*-hexane/*i*-PrOH = 80/20, detector: 230 nm, 30 °C, flow rate: 0.8 mL/min), *t*₁ = 12.1 min, *t*₂ = 13.2 min (major).

(-)-(*R*)-3-(3-Fluorophenyl)-3,4-dihydro-2H-benzo[b][1,4]oxazin-2-one (**6g**). 35 mg, 96% yield, white solid, known compound, *R*_f = 0.30 (hexane/ethyl acetate 10/1), 98% ee, [α]_D²⁰ = -128.71 (c 0.70, CHCl₃), [lit.:^{12b} [α]_D²⁰ = +100 (c 0.2, CHCl₃) for 89% ee]; ¹H NMR (400 MHz, CDCl₃) δ 7.36–7.29 (m, 1H), 7.19 (d, *J* = 7.8 Hz, 1H), 7.15–7.10 (m, 1H), 7.07–7.00 (m, 3H), 6.91–6.79 (m, 2H), 5.05 (d, *J* = 1.6 Hz, 1H), 4.32 (brs, 1H); ¹³C{¹H} NMR (100 MHz, CDCl₃) δ 164.7, 163.0 (d, ¹*J*_{F-C} = 246.0 Hz), 140.8, 138.7 (d, ³*J*_{F-C} = 6.9 Hz), 132.0, 130.6 (d, ³*J*_{F-C} = 8.1 Hz), 125.4, 123.2 (d, ⁴*J*_{F-C} = 3.1 Hz), 120.7, 117.0, 116.0 (d, ²*J*_{F-C} = 21.0 Hz), 115.0, 114.6 (d, ²*J*_{F-C} = 22.6 Hz), 58.8 (d, ⁴*J*_{F-C} = 1.8 Hz); ¹⁹F{¹H} NMR (376 MHz, CDCl₃) δ -111.53. HPLC (AD-H, elute: *n*-hexane/*i*-PrOH = 80/20, detector: 230 nm, 30 °C, flow rate: 0.8 mL/min), *t*₁ = 9.9 min, *t*₂ = 13.4 min (major).

(+)-(*R*)-3-(2-Methoxyphenyl)-3,4-dihydro-2H-benzo[b][1,4]oxazin-2-one (**6h**). 37 mg, 97% yield, yellow oil, known compound, *R*_f = 0.28 (hexane/ethyl acetate 10/1), 99% ee, [α]_D²⁰ = +151.88 (c 0.74, CHCl₃), [lit.:^{12b} [α]_D²⁰ = -110.5 (c 0.44, CHCl₃) for 48% ee]; ¹H NMR (400 MHz, CDCl₃) δ 7.33–7.27 (m, 1H), 7.22 (d, *J* = 6.6 Hz, 1H), 7.07–7.03 (m, 1H), 6.97–6.87 (m, 3H), 6.84–6.78 (m, 1H), 6.68–6.65 (m, 1H), 5.42 (s, 1H), 4.29 (brs, 1H), 3.82 (s, 3H); ¹³C{¹H} NMR (100 MHz, CDCl₃) δ 165.5, 157.1, 141.1, 132.5, 130.2, 128.2, 125.0, 124.9, 120.9, 120.0, 116.7, 115.1, 111.2, 55.7, 54.6. HPLC (AD-H, elute: *n*-hexane/*i*-PrOH = 80/20, detector: 230 nm, 30 °C, flow rate: 0.8 mL/min), *t*₁ = 12.4 min, *t*₂ = 16.3 min (major).

(-)-(*R*)-3-(3,4-Dimethylphenyl)-3,4-dihydro-2H-benzo[b][1,4]oxazin-2-one (**6i**). 35 mg, 92% yield, yellow solid, known compound, *R*_f = 0.50 (hexane/ethyl acetate 10/1), 97% ee, [α]_D²⁰ = -104.99 (c 0.70, CHCl₃), [lit.:^{8a} [α]_D¹⁶ = -85.1 (c 0.96, CHCl₃) for 90% ee]; ¹H NMR (400 MHz, CDCl₃) δ 7.16 (s, 1H), 7.13–7.06 (m, 2H), 7.05–6.96 (m, 2H), 6.87–6.81 (m, 1H), 6.80–6.75 (m, 1H), 4.95 (s, 1H), 4.22 (brs, 1H), 2.23 (s, 6H); ¹³C{¹H} NMR (100 MHz, CDCl₃) δ 165.6, 141.0, 137.6, 137.4, 133.8, 132.6, 130.2, 128.8, 125.1, 124.8, 120.3, 116.9, 114.9, 59.1, 19.9, 19.5. HPLC (OD-H, elute: *n*-hexane/*i*-PrOH = 70/30, detector: 230 nm, 30 °C, flow rate: 0.7 mL/min), *t*₁ = 12.9 min (major), *t*₂ = 28.5 min.

(-)-(*S*)-3-(Thiophen-2-yl)-3,4-dihydro-2H-benzo[b][1,4]oxazin-2-one (**6j**). 29 mg, 84% yield, yellow solid, known compound, *R*_f = 0.30 (hexane/ethyl acetate 10/1), 94% ee, [α]_D²⁰ = -40.17 (c 0.59, CHCl₃), [lit.:^{12b} [α]_D²⁰ = +32 (c 0.2, CHCl₃) for 86% ee]; ¹H NMR (400 MHz, CDCl₃) δ 7.26 (d, *J* = 5.2 Hz, 1H), 7.09–7.00 (m, 3H), 6.98–6.93 (m, 1H), 6.92–6.86 (m, 1H), 6.82 (d, *J* = 7.6 Hz, 1H), 5.36 (s, 1H), 4.39 (brs, 1H); ¹³C{¹H} NMR (100 MHz, CDCl₃) δ 164.1, 141.0, 138.7, 131.5, 127.1, 126.9, 126.5, 125.3, 120.9, 117.0, 115.5, 55.2. HPLC (AD-H, elute: *n*-hexane/*i*-PrOH = 80/20, detector: 230 nm, 30 °C, flow rate: 0.8 mL/min), *t*₁ = 12.0 min, *t*₂ = 28.1 min (major).

(-)-(*R*)-6-Methyl-3-phenyl-3,4-dihydro-2H-benzo[b][1,4]oxazin-2-one (**6k**). 35 mg, yellow oil, 97% yield, known compound, *R*_f = 0.30 (hexane/ethyl acetate 10/1), 99% ee, [α]_D²⁰ = -139.56 (c 0.70, CHCl₃), [lit.:^{8a} [α]_D¹⁶ = -104.9 (c 0.74, CHCl₃) for 87% ee]; ¹H NMR (400 MHz, CDCl₃) δ 7.41–7.32 (m, 5H), 6.90 (d, *J* = 8.2 Hz, 1H), 6.64 (d, *J* = 8.2 Hz, 1H), 6.60 (s, 1H), 5.01 (d, *J* = 1.2 Hz, 1H), 4.20 (brs, 1H), 2.27 (s, 3H); ¹³C{¹H} NMR (100 MHz, CDCl₃) δ 165.4, 138.9, 136.6, 135.1, 132.0, 129.0, 128.9, 127.5, 121.0, 116.6, 115.4, 59.3, 21.0. HPLC (OD-H, elute: *n*-hexane/*i*-PrOH = 70/30, detector: 230 nm, 30 °C, flow rate: 0.7 mL/min), *t*₁ = 9.6 min (major), *t*₂ = 12.4 min.

(-)-(*R*)-6-Chloro-3-phenyl-3,4-dihydro-2H-benzo[b][1,4]oxazin-2-one (**6l**). 38 mg, 97% yield, white solid, known compound, *R*_f = 0.50 (hexane/ethyl acetate 10/1), 99% ee, [α]_D²⁰ = -158.80 (c 0.76,

CHCl₃), [lit.^{8a} $[\alpha]_D^{15} = -109.9$ (c 0.90, CHCl₃) for 89% ee]; ¹H NMR (400 MHz, CDCl₃) δ 7.40–7.32 (m, 5H), 6.93 (d, $J = 8.2$ Hz, 1H), 6.84–6.75 (m, 2H), 5.05 (d, $J = 1.6$ Hz, 1H), 4.41 (brs, 1H); ¹³C{¹H} NMR (100 MHz, CDCl₃) δ 164.5, 139.3, 136.0, 133.2, 130.2, 129.2, 129.1, 127.3, 120.1, 118.0, 114.7, 58.8. HPLC (OD-H, elute: *n*-hexane/*i*-PrOH = 70/30, detector: 230 nm, 30 °C, flow rate: 0.7 mL/min), $t_1 = 10.3$ min (major), $t_2 = 14.8$ min.

(-)-(*R*)-3-Methyl-3,4-dihydro-2H-benzo[*b*][1,4]oxazin-2-one (**6m**). 20 mg, 83% yield, yellow oil, known compound, $R_f = 0.30$ (hexane/ethyl acetate 10/1), 97% ee, $[\alpha]_D^{20} = -41.00$ (c 0.40, CHCl₃), [lit.^{15b} $[\alpha]_D^{20} = -38.4$ (c 0.24, CHCl₃) for 97% ee]; ¹H NMR (400 MHz, CDCl₃) δ 7.04–6.95 (m, 2H), 6.89–6.80 (m, 1H), 6.80–6.76 (m, 1H), 4.02–3.84 (m, 1H; brs, 1H), 1.54 (d, $J = 6.6$ Hz, 3H); ¹³C{¹H} NMR (100 MHz, CDCl₃) δ 167.4, 141.4, 133.0, 125.0, 120.5, 116.9, 115.1, 50.6, 17.2. HPLC (OD-H, elute: *n*-hexane/*i*-PrOH = 70/30, detector: 230 nm, 30 °C, flow rate: 0.7 mL/min), $t_1 = 6.8$ min (major), $t_2 = 7.9$ min.

(-)-(*R*)-3-Ethyl-3,4-dihydro-2H-benzo[*b*][1,4]oxazin-2-one (**6n**). 24 mg, 92% yield, colorless oil, known compound, $R_f = 0.40$ (hexane/ethyl acetate 5/1), 98% ee, $[\alpha]_D^{20} = -51.04$ (c 0.48, CHCl₃), [lit.^{15b} $[\alpha]_D^{20} = -23.4$ (c 0.22, CHCl₃) for 79% ee]; ¹H NMR (400 MHz, CDCl₃) δ 6.99 (t, $J = 7.6$ Hz, 2H), 6.83 (t, $J = 7.7$ Hz, 1H), 6.78 (d, $J = 7.8$ Hz, 1H), 3.98 (brs, 1H), 3.90–3.85 (m, 1H), 2.03–1.89 (m, 1H), 1.89–1.77 (m, 1H), 1.07 (t, $J = 7.5$ Hz, 3H); ¹³C{¹H} NMR (100 MHz, CDCl₃) δ 166.6, 141.0, 132.5, 125.0, 120.2, 116.7, 115.1, 56.0, 24.5, 9.6. HPLC (OD-H, elute: *n*-hexane/*i*-PrOH = 90/10, detector: 230 nm, 30 °C, flow rate: 0.7 mL/min), $t_1 = 14.1$ min (major), $t_2 = 17.6$ min.

(-)-(*R*)-3-Butyl-3,4-dihydro-2H-benzo[*b*][1,4]oxazin-2-one (**6o**). 28 mg, 92% yield, yellow oil, known compound,^{9b} $R_f = 0.50$ (hexane/ethyl acetate 10/1), 99% ee, $[\alpha]_D^{20} = -43.75$ (c 0.56, CHCl₃), ¹H NMR (400 MHz, CDCl₃) δ 7.02–6.96 (m, 2H), 6.87–6.81 (m, 1H), 6.80–6.74 (m, 1H), 4.03–3.87 (m, 1H; brs, 1H), 1.98–1.86 (m, 1H), 1.83–1.70 (m, 1H), 1.52–1.31 (m, 4H), 0.92 (t, $J = 7.2$ Hz, 3H); ¹³C{¹H} NMR (100 MHz, CDCl₃) δ 166.7, 141.1, 132.4, 125.0, 120.2, 116.8, 115.1, 54.8, 30.9, 27.4, 22.4, 13.9. HPLC (OD-H, elute: *n*-hexane/*i*-PrOH = 95/5, detector: 230 nm, 30 °C, flow rate: 0.7 mL/min), $t_1 = 21.4$ min (major), $t_2 = 24.7$ min.

(-)-(*R*)-3-Phenethyl-3,4-dihydro-2H-benzo[*b*][1,4]oxazin-2-one (**6p**). 37 mg, 97% yield, yellow solid, known compound,^{9b} $R_f = 0.50$ (hexane/ethyl acetate 10/1), 99% ee, $[\alpha]_D^{20} = -12.84$ (c 0.74, CHCl₃), ¹H NMR (400 MHz, CDCl₃) δ 7.33–7.27 (m, 2H), 7.25–7.18 (m, 3H), 7.03–6.93 (m, 2H), 6.83 (t, $J = 7.7$ Hz, 1H), 6.68–6.62 (m, 1H), 3.97–3.86 (m, 1H), 3.79 (brs, 1H), 2.91–2.73 (m, 2H), 2.35–2.21 (m, 1H), 2.13–2.01 (m, 1H); ¹³C{¹H} NMR (100 MHz, CDCl₃) δ 166.5, 141.1, 140.4, 132.3, 128.8, 128.5, 126.5, 125.0, 120.4, 116.8, 115.3, 54.5, 32.7, 31.7. HPLC (OD-H, elute: *n*-hexane/*i*-PrOH = 70/30, detector: 230 nm, 30 °C, flow rate: 0.7 mL/min), $t_1 = 8.5$ min (major), $t_2 = 12.7$ min.

Procedures for Biomimetic Asymmetric Reduction of Benzoxazine. A mixture of [Ru(*p*-cymene)I₂]₂ (0.5 mg, 0.0005 mmol), bis(4-nitrophenyl) hydrogen phosphate **2b** (1.4 mg, 0.004 mmol), the NAD(P)H model (*R*)-**1f** (2.9 mg, 0.01 mmol), and benzoxazine **7** (0.10 mmol) in chloroform (2 mL) was stirred at room temperature for 5 min in a glovebox, and then, the mixture was transferred to an autoclave. Hydrogenation was performed at 40 °C under hydrogen gas (500 psi) for 48 h. After careful release of the hydrogen, the autoclave was opened and the reaction mixture was directly purified by column chromatography on silica gel using hexane and ethyl acetate as the eluent to give the reductive products **8**. The enantiomeric excesses were determined by chiral HPLC.

(-)-(*S*)-3-Phenyl-3,4-dihydro-2H-benzo[*b*][1,4]oxazine (**8**). 18 mg, 85% yield, yellow oil, known compound, $R_f = 0.70$ (hexane/ethyl acetate 20/1), 91% ee, $[\alpha]_D^{20} = -105.99$ (c 0.20, CHCl₃), [lit.^{15a} $[\alpha]_D^{RT} = -118.1$ (c 1.0, CHCl₃) for 98% ee]; ¹H NMR (400 MHz, CDCl₃) δ 7.43–7.30 (m, 5H), 6.89–6.76 (m, 2H), 6.72–6.64 (m, 2H), 4.53–4.45 (m, 1H), 4.30–4.24 (m, 1H), 4.03–3.95 (m, 1H; brs, 1H); ¹³C{¹H} NMR (100 MHz, CDCl₃) δ 143.1, 138.7, 133.4, 128.3, 127.9, 126.7, 121.0, 118.4, 116.1, 114.9, 70.5, 53.7. HPLC

(OD-H, elute: *n*-hexane/*i*-PrOH = 70/30, detector: 230 nm, 30 °C, flow rate: 0.7 mL/min), $t_1 = 11.6$ min (major), $t_2 = 15.4$ min.

Procedures for Biomimetic Asymmetric Reduction of Alkynyl Ketimines. A mixture of [Ru(*p*-cymene)I₂]₂ (0.5 mg, 0.0005 mmol), bis(4-nitrophenyl) hydrogen phosphate **2b** (1.4 mg, 0.004 mmol), the NAD(P)H model (*R*)-**1f** (2.9 mg, 0.01 mmol), and alkynyl ketimines **9a–c** (0.10 mmol) in chloroform (2 mL) was stirred at room temperature for 5 min in a glovebox, and then, the mixture was transferred to an autoclave. Hydrogenation was performed at 40 °C under hydrogen gas (500 psi) for 48 h. After careful release of hydrogen, the autoclave was opened and the reaction mixture was directly purified by column chromatography on silica gel using hexane and ethyl acetate as the eluent to give the products **10a–c**. The enantiomeric excesses were determined by chiral HPLC.

(+)-(*S*)-4-Methoxy-*N*-(1,1,1-trifluoro-4-phenylbut-3-yn-2-yl)-aniline (**10a**). 30 mg, 98% yield, yellow oil, known compound, $R_f = 0.60$ (hexane/ethyl acetate 20/1), 97% ee, $[\alpha]_D^{20} = +229.98$ (c 0.60, CHCl₃), [lit.^{8b} $[\alpha]_D^{20} = -231.28$ (c 1.16, CHCl₃) for 95% ee]; ¹H NMR (400 MHz, CDCl₃) δ 7.50–7.41 (m, 2H), 7.40–7.29 (m, 3H), 6.83 (dd, $J = 21.2, 8.8$ Hz, 4H), 4.84–4.72 (m, 1H), 3.79 (s, 3H; brs, 1H); ¹³C{¹H} NMR (100 MHz, CDCl₃) δ 154.4, 139.1, 132.2, 129.3, 128.6, 124.0 (q, $J = 280.0$ Hz), 121.6, 117.1, 115.1, 86.5, 81.0 (q, $J = 2.3$ Hz), 55.9, 52.4 (q, $J = 33.8$ Hz); ¹⁹F{¹H} NMR (376 MHz, CDCl₃) δ -75.69. HPLC (AD-H, elute: *n*-hexane/*i*-PrOH = 95/5, detector: 254 nm, 30 °C, flow rate: 0.8 mL/min), $t_1 = 15.2$ min (major), $t_2 = 16.1$ min.

(+)-(*S*)-4-Methoxy-*N*-(1,1,1-trifluoro-4-(*p*-tolyl)but-3-yn-2-yl)-aniline (**10b**). 31 mg, 97% yield, yellow oil, known compound, $R_f = 0.60$ (hexane/ethyl acetate 10/1), 93% ee, $[\alpha]_D^{20} = +231.82$ (c 0.60, CHCl₃), [lit.^{8b} $[\alpha]_D^{20} = -288.76$ (c 0.90, CHCl₃) for 95% ee]; ¹H NMR (400 MHz, CDCl₃) δ 7.24 (d, $J = 8.1$ Hz, 2H), 7.03 (d, $J = 7.9$ Hz, 2H), 6.80–6.73 (m, 2H), 6.73–6.67 (m, 2H), 4.71–4.61 (m, 1H), 3.69 (s, 3H), 3.66 (brs, 1H), 2.26 (s, 3H); ¹³C{¹H} NMR (100 MHz, CDCl₃) δ 154.2, 139.4, 139.0, 131.9, 129.1, 123.8 (q, $J = 279.9$ Hz), 118.4, 116.9, 114.9, 86.5, 80.2 (q, $J = 2.3$ Hz), 55.7, 52.2 (q, $J = 33.7$ Hz), 21.5; ¹⁹F{¹H} NMR (376 MHz, CDCl₃) δ -75.74. HPLC (AS-H, elute: *n*-hexane/*i*-PrOH = 95/5, detector: 254 nm, 30 °C, flow rate: 0.8 mL/min), $t_1 = 9.7$ min (major), $t_2 = 10.7$ min.

(+)-(*S*)-4-Methoxy-*N*-(1,1,1-trifluoro-4-(4-fluorophenyl)but-3-yn-2-yl)-aniline (**10c**). 30 mg, 93% yield, yellow oil, known compound, $R_f = 0.50$ (hexane/ethyl acetate 10/1), 99% ee, $[\alpha]_D^{20} = +203.65$ (c 0.60, CHCl₃), [lit.^{8b} $[\alpha]_D^{20} = -204.91$ (c 1.26, CHCl₃) for 95% ee]; ¹H NMR (400 MHz, CDCl₃) δ 7.38–7.29 (m, 2H), 6.97–6.88 (m, 2H), 6.80–6.74 (m, 2H), 6.73–6.67 (m, 2H), 4.71–4.62 (m, 1H), 3.70–3.62 (s, 3H; brs, 1H); ¹³C{¹H} NMR (100 MHz, CDCl₃) δ 163.0 (d, ¹*J*_{F-C} = 249.2 Hz), 154.2, 138.8, 134.0 (d, ³*J*_{F-C} = 8.5 Hz), 123.7 (q, $J = 279.9$ Hz), 117.5 (d, ⁴*J*_{F-C} = 3.5 Hz), 116.9, 115.7 (d, ²*J*_{F-C} = 22.1 Hz), 114.9, 85.2, 80.7, 55.7, 52.1 (q, $J = 33.8$ Hz); ¹⁹F{¹H} NMR (376 MHz, CDCl₃) δ -75.67, -109.39. HPLC (AS-H, elute: *n*-hexane/*i*-PrOH = 95/5, detector: 254 nm, 30 °C, flow rate: 0.8 mL/min), $t_1 = 12.1$ min (major), $t_2 = 18.5$ min.

Procedures for Biomimetic Asymmetric Reduction of Quinolines. A mixture of [Ru(*p*-cymene)I₂]₂ (0.5 mg, 0.0005 mmol), bis(4-nitrophenyl) hydrogen phosphate **2b** (1.4 mg, 0.004 mmol), the NAD(P)H model (*R*)-**1f** (2.9 mg, 0.01 mmol), and quinolines **11a–c** (0.10 mmol) in chloroform (1.50 mL)/tetrahydrofuran (THF) (0.50 mL) was stirred at room temperature for 5 min in a glovebox, and then, the mixture was transferred to an autoclave. Hydrogenation was performed at 40 °C under hydrogen gas (500 psi) for 48 h. After careful release of the hydrogen gas, the autoclave was opened and the reaction mixture was directly purified by column chromatography on silica gel using hexanes and ethyl acetate as the eluent to give **12a–c**. The enantiomeric excesses were determined by chiral HPLC.

(-)-(*S*)-2-Phenyl-1,2,3,4-tetrahydroquinoline (**12a**). 20 mg, 96% yield, yellow solid, known compound, $R_f = 0.70$ (hexane/ethyl acetate 20/1), 83% ee, $[\alpha]_D^{20} = -23.50$ (c 0.40, CHCl₃), [lit.^{8a} $[\alpha]_D^{19} = -35.7$ (c 0.80, CHCl₃) for 91% ee]; ¹H NMR (400 MHz, CDCl₃) δ 7.49–7.37 (m, 4H), 7.37–7.30 (m, 1H), 7.10–7.02 (m, 2H), 6.70 (t, $J = 7.3$ Hz, 1H), 6.58 (d, $J = 7.9$ Hz, 1H), 4.48 (d, $J = 7.6$ Hz, 1H), 4.07 (brs, 1H), 3.03–2.91 (m, 1H), 2.83–2.74 (m, 1H), 2.23–2.12

(m, 1H), 2.10–1.98 (m, 1H); $^{13}\text{C}\{^1\text{H}\}$ NMR (100 MHz, CDCl_3) δ 145.0, 144.9, 129.5, 128.8, 127.6, 127.1, 126.7, 121.1, 117.3, 114.2, 56.4, 31.2, 26.6. HPLC (AS-H, elute: *n*-hexane/*i*-PrOH = 85/15, detector: 254 nm, 30 °C, flow rate: 0.7 mL/min), t_1 = 8.1 min, t_2 = 17.5 min (major).

(–)-(S)-2-(4-Chlorophenyl)-1,2,3,4-tetrahydroquinoline (**12b**). 24 mg, 99% yield, white solid, known compound, R_f = 0.70 (hexane/ethyl acetate 20/1), 83% ee, $[\alpha]_{\text{D}}^{20}$ = –35.41 (c 0.48, CHCl_3), [lit.:^{8a} $[\alpha]_{\text{D}}^{20}$ = –36.0 (c 0.92, CHCl_3) for 91% ee]; ^1H NMR (400 MHz, CDCl_3) δ 7.33–7.27 (m, 4H), 7.04–6.95 (m, 1H), 6.69–6.62 (m, 1H), 6.56–6.62 (t, J = 7.3 Hz, 1H), 6.53 (d, J = 7.9 Hz, 1H), 4.43–4.37 (m, 1H), 3.98 (brs, 1H), 2.95–2.85 (m, 1H), 2.74–2.65 (m, 1H), 2.12–2.04 (m, 1H), 1.99–1.87 (m, 1H); $^{13}\text{C}\{^1\text{H}\}$ NMR (100 MHz, CDCl_3) δ 144.6, 143.5, 133.2, 129.5, 128.9, 128.1, 127.2, 121.0, 117.6, 114.3, 55.8, 31.2, 26.3. HPLC (AS-H, elute: *n*-hexane/*i*-PrOH = 85/15, detector: 254 nm, 30 °C, flow rate: 0.8 mL/min), t_1 = 8.4 min, t_2 = 16.9 min (major).

(–)-(S)-2-(3-Bromophenyl)-1,2,3,4-tetrahydroquinoline (**12c**). 27 mg, 94% yield, yellow oil, known compound, R_f = 0.60 (hexane/ethyl acetate 20/1), 90% ee, $[\alpha]_{\text{D}}^{20}$ = –39.63 (c 0.54, CHCl_3), [lit.:^{18d} $[\alpha]_{\text{D}}^{\text{RT}}$ = –46.6 (c 1.0, CHCl_3) for 98% ee]; ^1H NMR (400 MHz, CDCl_3) δ 7.46 (t, J = 1.6 Hz, 1H), 7.35–7.29 (m, 1H), 7.22 (d, J = 7.7 Hz, 1H), 7.12 (t, J = 7.8 Hz, 1H), 6.96–6.88 (m, 2H), 6.61–6.54 (m, 1H), 6.46 (d, J = 7.9 Hz, 1H), 4.31 (dd, J = 9.2, 3.3 Hz, 1H), 3.92 (brs, 1H), 2.87–2.75 (m, 1H), 2.69–2.58 (m, 1H), 2.06–1.96 (m, 1H), 1.94–1.81 (m, 1H); $^{13}\text{C}\{^1\text{H}\}$ NMR (100 MHz, CDCl_3) δ 147.4, 144.5, 130.7, 130.3, 129.8, 129.5, 127.2, 125.4, 122.9, 121.0, 117.6, 114.3, 55.9, 31.2, 26.3. HPLC (AS-H, elute: *n*-hexane/*i*-PrOH = 90/10, detector: 254 nm, 30 °C, flow rate: 0.8 mL/min), t_1 = 7.8 min, t_2 = 17.2 min (major).

ASSOCIATED CONTENT

Supporting Information

The Supporting Information is available free of charge at <https://pubs.acs.org/doi/10.1021/acs.joc.9b03054>.

Mechanistic investigation including isotopic-labeling experiments and density functional theory calculation; NMR spectra and HPLC spectra of products (PDF)

X-ray crystallography data of (R)-**1c** (CCDC 1813610) (CIF)

X-ray crystallography data of (S)-**1e** (CCDC 1815222) (CIF)

AUTHOR INFORMATION

Corresponding Authors

Yi Luo – Dalian University of Technology, Dalian, P. R. China; orcid.org/0000-0001-6390-8639; Email: luoyi@dlut.edu.cn

Yong-Gui Zhou – Dalian Institute of Chemical Physics, Chinese Academy of Sciences, Dalian, P. R. China, and Dalian University of Technology, Dalian, P. R. China; orcid.org/0000-0002-3321-5521; Email: ygzhou@dicp.ac.cn

Other Authors

Jie Wang – Dalian Institute of Chemical Physics, Chinese Academy of Sciences, Dalian, P. R. China

Zi-Biao Zhao – Dalian Institute of Chemical Physics, Chinese Academy of Sciences, Dalian, P. R. China

Yanan Zhao – Dalian University of Technology, Dalian, P. R. China; orcid.org/0000-0002-3928-3429

Gen Luo – Dalian University of Technology, Dalian, P. R. China; orcid.org/0000-0002-5297-6756

Zhou-Hao Zhu – Dalian Institute of Chemical Physics, Chinese Academy of Sciences, Dalian, P. R. China; orcid.org/0000-0002-5227-5669

Complete contact information is available at: <https://pubs.acs.org/doi/10.1021/acs.joc.9b03054>

Author Contributions

[§]J.W. and Z.-B.Z. contributed equally to this work.

Notes

The authors declare no competing financial interest.

ACKNOWLEDGMENTS

Financial support from the National Natural Science Foundation of China (21532006 and 21690074) and Chinese Academy of Sciences (XDB17020300) is acknowledged. We also thank the Fundamental Research Funds for the Central Universities (DUT18RC3002 and DUT18GJ201) and the Network and Information Center of Dalian University of Technology for the computational resources.

REFERENCES

- (1) (a) Gebicki, J.; Marcinek, A.; Zielonka, J. Transient species in the stepwise interconversion of NADH and NAD⁺. *Acc. Chem. Res.* **2004**, *37*, 379–386. (b) Houtkooper, R. H.; Cantó, C.; Wanders, R. J.; Auwerx, J. The secret life of NAD⁺: an old metabolite controlling new metabolic signaling pathways. *Endocr. Rev.* **2010**, *31*, 194–223. (c) Lin, H. Nicotinamide adenine dinucleotide: beyond a redox coenzyme. *Org. Biomol. Chem.* **2007**, *5*, 2541–2554. (d) Wu, H.; Tian, C.; Song, X.; Liu, C.; Yang, D.; Jiang, Z. Methods for the regeneration of nicotinamide coenzymes. *Green Chem.* **2013**, *15*, 1773–1789.
- (2) For selected reviews and papers on chiral NAD(P)H models, see: (a) Wang, N.-X.; Zhao, J. Progress in coenzyme NADH model compounds and asymmetric reduction of benzoylformate. *Synlett* **2007**, *2007*, 2785–2791. (b) Bai, C.-B.; Wang, N.-X.; Xing, Y.; Lan, X.-W. Progress on chiral NAD(P)H model compounds. *Synlett* **2017**, *28*, 402–414. (c) Ohnishi, Y.; Kagami, M.; Ohno, A. Reduction by a model of NAD(P)H. Effect of metal ion and stereochemistry on the reduction of α -keto esters by 1,4-dihydropyridinone derivatives. *J. Am. Chem. Soc.* **1975**, *97*, 4766–4768. (d) Kanomata, N.; Nakata, T. A compact chemical miniature of a holoenzyme, coenzyme NADH linked dehydro-genase. Design and synthesis of bridged NADH models and their highly enantioselective reduction. *J. Am. Chem. Soc.* **2000**, *122*, 4563–4568.
- (3) For selected reviews on Hantzsch ester-mediated biomimetic asymmetric reduction, see: (a) Ouellet, S. G.; Walji, A. M.; Macmillan, D. W. C. Enantioselective organocatalytic transfer hydrogenation reactions using Hantzsch esters. *Acc. Chem. Res.* **2007**, *40*, 1327–1339. (b) Zheng, C.; You, S.-L. Transfer hydrogenation with Hantzsch esters and related organic hydride donors. *Chem. Soc. Rev.* **2012**, *41*, 2498–2518. (c) Rueping, M.; Dufour, J.; Schoepke, F. R. Advances in catalytic metal-free reductions: from bio-inspired concepts to applications in the organocatalytic synthesis of pharmaceuticals and natural products. *Green Chem.* **2011**, *13*, 1084–1105. (d) Phillips, A. M. F.; Pombeiro, A. J. L. Recent advances in organocatalytic enantioselective transfer hydrogenation. *Org. Biomol. Chem.* **2017**, *15*, 2307–2340.
- (4) Zhu, C.; Saito, K.; Yamanaka, M.; Akiyama, T. Benzothiazoline: versatile hydrogen donor for organocatalytic transfer hydrogenation. *Acc. Chem. Res.* **2015**, *48*, 388–398.
- (5) For selected papers on the organocatalyst-catalyzed asymmetric reactions, see: (a) Singh, S.; Batra, U. K. Asymmetric reductions of imines using NADH models. *Indian J. Chem., Sect. B: Org. Chem. Incl. Med. Chem.* **1989**, *28*, 1–2. (b) Yang, J. W.; Hechavarria Fonseca, M. T. H.; List, B. A metal-free transfer hydrogenation: organocatalytic conjugate reduction of α,β -unsaturated aldehydes. *Angew. Chem., Int.*

Ed. **2004**, *43*, 6660–6662. (c) Rueping, M.; Sugiono, E.; Azap, C.; Theissmann, T.; Bolte, M. Enantioselective Brønsted acid catalyzed transfer hydrogenation: organocatalytic reduction of imines. *Org. Lett.* **2005**, *7*, 3781–3783. (d) Yang, J. W.; Hechavarría Fonseca, M. T.; Vignola, N.; List, B. Metal-free, organocatalytic asymmetric transfer hydrogenation of α,β -unsaturated aldehydes. *Angew. Chem., Int. Ed.* **2005**, *44*, 108–110. (e) Ouellet, S. G.; Tuttle, J. B.; MacMillan, D. W. C. Enantioselective organocatalytic hydride reduction. *J. Am. Chem. Soc.* **2005**, *127*, 32–33. (f) Hoffmann, S.; Seayad, A. M.; List, B. A powerful Brønsted acid catalyst for the organocatalytic asymmetric transfer hydrogenation of imines. *Angew. Chem., Int. Ed.* **2005**, *44*, 7424–7427. (g) Wang, Z.; Ai, F.; Wang, Z.; Zhao, W.; Zhu, G.; Lin, Z.; Sun, J. Organocatalytic asymmetric synthesis of 1,1-diarylethanes by transfer hydrogenation. *J. Am. Chem. Soc.* **2015**, *137*, 383–389. (h) Mayer, S.; List, B. Asymmetric counteranion-directed catalysis. *Angew. Chem., Int. Ed.* **2006**, *45*, 4193–4195. (i) Martin, N. J. A.; List, B. Highly enantioselective transfer hydrogenation of α,β -unsaturated ketones. *J. Am. Chem. Soc.* **2006**, *128*, 13368–13369.

(6) For selected papers on the metal-catalyzed asymmetric reactions, see: (a) Zehani, S.; Gelbard, G. Asymmetric reductions catalyzed by chiral shift reagents. *J. Chem. Soc., Chem. Commun.* **1985**, 1162–1163. (b) Yang, J. W.; List, B. Catalytic asymmetric transfer hydrogenation of α -ketoesters with Hantzsch esters. *Org. Lett.* **2006**, *8*, 5653–5655. (c) Wang, D.-W.; Zeng, W.; Zhou, Y.-G. Iridium-catalyzed asymmetric transfer hydrogenation of quinolines with Hantzsch esters. *Tetrahedron: Asymmetry* **2007**, *18*, 1103–1107.

(7) For selected papers on regeneration of NAD(P)H models, see (a) Lo, H. C.; Fish, R. H. Biomimetic NAD⁺ models for tandem cofactor regeneration, horse liver alcohol dehydrogenase recognition of 1,4-NADH derivatives, and chiral synthesis. *Angew. Chem., Int. Ed.* **2002**, *41*, 478–481. (b) Xu, H.-J.; Liu, Y.-C.; Fu, Y.; Wu, Y.-D. Catalytic hydrogenation of α,β -epoxy ketones to form β -hydroxy ketones mediated by an NADH coenzyme model. *Org. Lett.* **2006**, *8*, 3449–3451. (c) Procuranti, B.; Connon, S. J. A reductase-mimicking thiourea organocatalyst incorporating a covalently bound NADH analogue: efficient 1,2-diketone reduction with in situ prosthetic group generation and recycling. *Chem. Commun.* **2007**, 1421–1423. (d) Chen, Q.-A.; Chen, M.-W.; Yu, C.-B.; Shi, L.; Wang, D.-S.; Yang, Y.; Zhou, Y.-G. Biomimetic asymmetric hydrogenation: in situ regenerable Hantzsch esters for asymmetric hydrogenation of benzoxazinones. *J. Am. Chem. Soc.* **2011**, *133*, 16432–16435. (e) Zhao, L.; Wei, J.; Lu, J.; He, C.; Duan, C. Renewable molecular flasks with NADH models: combination of light-driven proton reduction and biomimetic hydrogenation of benzoxazinones. *Angew. Chem., Int. Ed.* **2017**, *56*, 8692–8696.

(8) (a) Chen, Q.-A.; Gao, K.; Duan, Y.; Ye, Z.-S.; Shi, L.; Yang, Y.; Zhou, Y.-G. Dihydrophenanthridine: a new and easily regenerable NAD(P)H model for biomimetic asymmetric hydrogenation. *J. Am. Chem. Soc.* **2012**, *134*, 2442–2448. (b) Chen, M.-W.; Wu, B.; Chen, Z.-P.; Shi, L.; Zhou, Y.-G. Synthesis of chiral fluorinated propargylamines via chemoselective biomimetic hydrogenation. *Org. Lett.* **2016**, *18*, 4650–4653. (c) Chen, Z.-P.; Chen, M.-W.; Guo, R.-N.; Zhou, Y.-G. 4,5-Dihydropyrrolo[1,2-a]quinoxalines: a tunable and regenerable biomimetic hydrogen source. *Org. Lett.* **2014**, *16*, 1406–1409.

(9) (a) Lu, L.-Q.; Li, Y.; Junge, K.; Beller, M. Iron-catalyzed hydrogenation for the in situ regeneration of an NAD(P)H model: biomimetic reduction of α -keto-/ α -iminoesters. *Angew. Chem., Int. Ed.* **2013**, *52*, 8382–8386. (b) Lu, L.-Q.; Li, Y.; Junge, K.; Beller, M. Relay iron/chiral Brønsted acid catalysis: enantioselective hydrogenation of benzoxazinones. *J. Am. Chem. Soc.* **2015**, *137*, 2763–2768.

(10) Wang, J.; Zhu, Z.-H.; Chen, M.-W.; Chen, Q.-A.; Zhou, Y.-G. Catalytic biomimetic asymmetric reduction of alkenes and imines enabled by chiral and regenerable NAD(P)H models. *Angew. Chem., Int. Ed.* **2019**, *58*, 1813–1817.

(11) (a) The procedures of the synthesis of axially chiral NAD(P)H model **1b–e** were provided in Supporting Information. (b) CCDC 1813610 and CCDC 1815222 contain supplementary crystallographic data of (–)-**1c** and (+)-**1e**.

(12) (a) Rueping, M.; Tato, F.; Schoepke, F. R. The first general, efficient and highly enantioselective reduction of quinoxalines and quinoxalinones. *Chem. – Eur. J.* **2010**, *16*, 2688–2691. (b) Xue, Z.-Y.; Jiang, Y.; Peng, X.-Z.; Yuan, W.-C.; Zhang, X.-M. The first general, highly enantioselective Lewis base organo-catalyzed hydrosilylation of benzoxazinones and quinoxalinones. *Adv. Synth. Catal.* **2010**, *352*, 2132–2136.

(13) (a) Kealy, T. J.; Pauson, P. L. A new type of organo-iron compound. *Nature* **1951**, *168*, 1039–1040. (b) Miller, S. A.; Tebboth, J. F.; Tremaine, J. F. Dicyclopentadienyliron. *J. Chem. Soc.* **1952**, 632–635. (c) Fu, G. C. Enantioselective nucleophilic catalysis with “planar-chiral” heterocycles. *Acc. Chem. Res.* **2000**, *33*, 412–420. (d) Dai, L.-X.; Tu, T.; You, S.-L.; Deng, W.-P.; Hou, X.-L. Asymmetric catalysis with chiral ferrocene ligands. *Acc. Chem. Res.* **2003**, *36*, 659–667. (e) Colacot, T. J. A concise update on the applications of chiral ferrocenyl phosphines in homogeneous catalysis leading to organic synthesis. *Chem. Rev.* **2003**, *103*, 3101–3118. (f) Fu, G. C. Asymmetric catalysis with “planar-chiral” derivatives of 4-(dimethylamino)pyridine. *Acc. Chem. Res.* **2004**, *37*, 542–547. (g) Arrayás, R. G.; Adrio, J.; Carretero, J. C. Recent applications of chiral ferrocene ligands in asymmetric catalysis. *Angew. Chem., Int. Ed.* **2006**, *45*, 7674–7715. (h) Dai, L.-X.; Hou, X.-L., Eds. *Chiral Ferrocenes in Asymmetric Catalysis*; Wiley: Weinheim, Germany, 2010. (i) Schaarschmidt, D.; Lang, H. Selective syntheses of planar-chiral ferrocenes. *Organometallics* **2013**, *32*, 5668–5704. (j) Gao, D.-W.; Gu, Q.; Zheng, C.; You, S.-L. Synthesis of planar chiral ferrocenes via transition-metal-catalyzed direct C–H bond functionalization. *Acc. Chem. Res.* **2017**, *50*, 351–365.

(14) Riant, O.; Samuel, O.; Kagan, H. B. A general asymmetric synthesis of ferrocenes with planar chirality. *J. Am. Chem. Soc.* **1993**, *115*, 5835–5836.

(15) (a) Rueping, M.; Antonchick, A. P.; Theissmann, T. Remarkably low catalyst loading in Brønsted acid catalyzed transfer hydrogenations: enantioselective reduction of benzoxazines, benzothiazines, and benzoxazinones. *Angew. Chem., Int. Ed.* **2006**, *45*, 6751–6755. (b) Storer, R. L.; Carrera, D. E.; Ni, Y.; MacMillan, D. W. C. Enantioselective organocatalytic reductive amination. *J. Am. Chem. Soc.* **2006**, *128*, 84–86. (c) Macías, F. A.; Marín, D.; Oliveros-Bastidas, A.; Molinillo, J. M. G. Rediscovering the biochemical and ecological role of 1,4-benzoxazinones. *Nat. Prod. Rep.* **2009**, *26*, 478–489.

(16) (a) Zhang, Z.; Ji, Y. R.; Wojtas, L.; Gao, W.-Y.; Ma, S.; Zaworotko, M. J.; Antilla, J. C. Two homochiral organocatalytic metal organic materials with nanoscopic channels. *Chem. Commun.* **2013**, *49*, 7693–7695. (b) Kundu, D. S.; Schmidt, J.; Bleschke, C.; Thomas, A.; Blechert, S. A microporous binol-derived phosphoric acid. *Angew. Chem., Int. Ed.* **2012**, *51*, 5456–5459. (c) Yang, Z.; Chen, F.; Zhang, S.; He, Y.; Yang, N.; Fan, Q.-H. Ruthenium-catalyzed enantioselective hydrogenation of phenanthridine derivatives. *Org. Lett.* **2017**, *19*, 1458–1461. (d) Rueping, M.; Sugiono, E.; Steck, A.; Theissmann, T. Synthesis and application of polymer-supported chiral Brønsted acid organo-catalysts. *Adv. Synth. Catal.* **2010**, *352*, 281–287.

(17) Kang, Q.; Zhao, Z.-A.; You, S.-L. Asymmetric transfer hydrogenation of β,γ -alkynyl α -imino esters by a Brønsted acid. *Org. Lett.* **2008**, *10*, 2031–2034.

(18) For selected reviews and papers on the asymmetric (transfer) hydrogenation of heteroaromatic compounds, see: (a) Glorius, F. Asymmetric hydrogenation of aromatic compounds. *Org. Biomol. Chem.* **2005**, *3*, 4171–4175. (b) Zhou, Y.-G. Asymmetric hydrogenation of heteroaromatic compounds. *Acc. Chem. Res.* **2007**, *40*, 1357–1366. (c) Kuwano, R. Catalytic asymmetric hydrogenation of 5-membered heteroaromatics. *Heterocycles* **2008**, *76*, 909–922. (d) Rueping, M.; Antonchick, A. P.; Theissmann, T. A highly enantioselective Brønsted acid catalyzed cascade reaction: organocatalytic transfer hydrogenation of quinolines and their application in the synthesis of alkaloids. *Angew. Chem., Int. Ed.* **2006**, *45*, 3683–3686. (e) Guo, Q.-S.; Du, D.-M.; Xu, J. The development of double axially chiral phosphoric acids and their catalytic transfer hydro-

genation of quinolines. *Angew. Chem., Int. Ed.* **2008**, *47*, 759–762; Corrigendum: *Angew. Chem., Int. Ed.* **2008**, *47*, 1541. (f) Tu, X.-F.; Gong, L.-Z. Highly enantioselective transfer hydrogenation of quinolines catalyzed by gold phosphates: achiral ligand tuning and chiral-anion control of stereoselectivity. *Angew. Chem., Int. Ed.* **2012**, *51*, 11346–11349. (g) Wang, W.-B.; Lu, S.-M.; Yang, P.-Y.; Han, X.-W.; Zhou, Y.-G. Highly enantioselective iridium-catalyzed hydrogenation of heteroaromatic compounds, quinolines. *J. Am. Chem. Soc.* **2003**, *125*, 10536–10537. (h) Shugrue, C. R.; Miller, S. J. Phosphothreonine as a catalytic residue in peptide-mediated asymmetric transfer hydrogenations of 8-aminoquinolines. *Angew. Chem., Int. Ed.* **2015**, *54*, 11173–11176. (i) Cai, X.-F.; Chen, M.-W.; Ye, Z.-S.; Guo, R.-N.; Shi, L.; Li, Y.-Q.; Zhou, Y.-G. Asymmetric transfer hydrogenation of 3-nitroquinolines: facile access to cyclic nitro compounds with two contiguous stereocenters. *Chem. Asian J.* **2013**, *8*, 1381–1385. (j) Wang, J.; Chen, M.-W.; Ji, Y.; Hu, S.-B.; Zhou, Y.-G. Kinetic resolution of axially chiral 5- or 8-substituted quinolines via asymmetric transfer hydrogenation. *J. Am. Chem. Soc.* **2016**, *138*, 10413–10416. (k) Chen, M.-W.; Cai, X.-F.; Chen, Z.-P.; Shi, L.; Zhou, Y.-G. Facile construction of three contiguous stereogenic centers via dynamic kinetic resolution in asymmetric transfer hydrogenation of quinolines. *Chem. Commun.* **2014**, *50*, 12526–12529.

(19) (a) Santelli, M.; Pons, J.-M. *Lewis Acids and Selectivity in Organic Synthesis*; CRC Press, 1995. (b) Kobayashi, S.; Manabe, K. Development of novel Lewis acid catalysts for selective organic reactions in aqueous media. *Acc. Chem. Res.* **2002**, *35*, 209–217.

(20) (a) Kraft, S.; Ryan, K.; Kargbo, R. B. Recent advances in asymmetric hydrogenation of tetrasubstituted olefins. *J. Am. Chem. Soc.* **2017**, *139*, 11630–11641. (b) Schrems, M. G.; Neumann, E.; Pfaltz, A. Iridium-catalyzed asymmetric hydrogenation of unfunctionalized tetrasubstituted olefins. *Angew. Chem., Int. Ed.* **2007**, *46*, 8274–8276. (c) Liu, Y.-T.; Chen, J.-Q.; Li, L.-P.; Shao, X.-Y.; Xie, J.-H.; Zhou, Q.-L. Asymmetric hydrogenation of tetrasubstituted cyclic enones to chiral cycloalkanols with three contiguous stereocenters. *Org. Lett.* **2017**, *19*, 3231–3234. (d) Liu, Y.-T.; Li, L.-P.; Xie, J.-H.; Zhou, Q.-L. Divergent asymmetric total synthesis of mulinane diterpenoids. *Angew. Chem., Int. Ed.* **2017**, *56*, 12708–12711.

(21) (a) Simón, L.; Goodman, J. M. Theoretical study of the mechanism of Hantzsch ester hydrogenation of imines catalyzed by chiral BINOL-phosphoric acids. *J. Am. Chem. Soc.* **2008**, *130*, 8741–8747. (b) Marcelli, T.; Hammar, P.; Himo, F. Phosphoric acid catalyzed enantioselective transfer hydrogenation of imines: a density functional theory study of reaction mechanism and the origins of enantioselectivity. *Chem. – Eur. J.* **2008**, *14*, 8562–8571.

(22) Zhang, Y.; Zhao, R.; Bao, R. L.-Y.; Shi, L. Highly enantioselective SPINOL-derived phosphoric acid catalyzed transfer hydrogenation of diverse C=N-containing heterocycles. *Eur. J. Org. Chem.* **2015**, 3344–3351.

(23) Zhang, L.; Qiu, R.; Xue, X.; Pan, Y.; Xu, C.; Li, H.; Xu, L. Versatile (pentamethylcyclopentadienyl)-rhodium-2,2'-bipyridine (Cp**Rh*-bpy) catalyst for transfer hydrogenation of N-heterocycles in water. *Adv. Synth. Catal.* **2015**, *357*, 3529–3537.